The *Nematostella* Wnt/β-catenin destruction complex provides insight into the evolution of the regulation of a major metazoan signal transduction pathway

Hongyan Sun[1,†], Radim Zidek[2], Mark Q. Martindale[2] and Athula Wikramanayake[1*]

[1]Department of Biology, University of Miami, Coral Gables, FL, 33146

[2]Whitney Laboratory for Marine Bioscience, 9505 Ocean Shore Blvd. St. Augustine, FL 32080-8610

[†] Current address: Pennington Biomedical Research Center, Baton Rouge, LA, 70808

[*]Corresponding author (athula@miami.edu)

Abstract

The Wnt/β-catenin (cWnt) signaling pathway is one of the most important intercellular signaling pathways in animals. How cWnt components regulate the pathway in bilaterians is well understood, but these processes are poorly characterized in the earliest branching animal clades. We used the cnidarian *Nematostella* (cnidarians are the closest bilaterian outgroup) to study the cWnt destruction complex (DC) which is the primary mechanism for regulating cytoplasmic concentrations of β-catenin. In bilaterians the DC scaffolding proteins Axin and APC directly interact and bind β-catenin to target it for proteolysis, but all non-bilaterian Axin and APC homologs lack the conserved domains required for bilaterian DC function. Using functional approaches, we show that in *Nematostella* Axin and APC-like proteins scaffold an active DC that is regulated differently than the bilaterian DC. Additionally, using AlphaFold software we discovered a sequence embedded in the Axin-RGS domain of non-bilaterian Axin that has homology to the bilaterian Axin β-catenin-binding motif (βcatBM). We propose that the bilaterian βcatBM evolved as a low-affinity β-catenin-interacting sequence in the Axin-RGS domain in pre-bilaterians and moved C-terminally in bilaterians where it acquired higher affinity for β-catenin. Our work provides novel insight into how regulatory modules can evolve in metazoan signaling pathways.

Introduction

The Wnt/β-catenin (cWnt) signaling pathway is a metazoan-specific pathway that plays diverse roles during evolution, development, and homeostasis[1–5]. Like most metazoan signaling pathways, the cWnt pathway is modular in its organization with distinct protein complexes regulating the flow of information from the cell surface to the nucleus[6–10] (Fig. 1A). β-catenin itself is involved in multiple cell biological functions, including a critical role in cell-cell adhesion, as well as in a role as a transcriptional co-factor in the cWnt pathway involved in cell fate specification[11] (Fig. 1A). These two deeply conserved roles of β-catenin have implicated it in major events in animal evolution including the evolution of multicellularity, segregation of primary germ layers and establishment of the primary body axis[3,12–15]. Thus, a better understanding of its cellular regulation in early emerging taxa is critical to gain insight into how cWnt contributed to the evolution and diversification of metazoans.

One critical regulatory module in the cWnt pathway that controls cytoplasmic β-catenin levels through targeted proteolysis is the cWnt destruction complex (DC)[8,16–18]. The two critical scaffolding proteins in the bilaterian DC that capture β-catenin from the cytoplasm are Axin and the tumor suppressor APC, the product of the Adenomatous Polyposis Coli gene (Fig. 1A). Axin has binding sites that mediate its direct association with proteins in the DC including β-catenin, Casein Kinase 1α (CK-1α), Glycogen Synthase Kinase 3β (GSK-3β), the phosphoprotein Disheveled, and APC[17–22] (Fig. 1B). APC is a relatively large protein with multiple domains that have been shown to mediate its interactions with Axin, β-catenin, and several other proteins[16,18,23,24] (Fig. 1C). Strikingly, APC has multiple distinct binding sites for β-catenin that have different affinities for the protein[16,23,24] (Fig. 1C). A model for negative regulation of β-catenin in

the cWnt pathway by the DC has emerged from extensive structure-function studies done in vertebrate and invertebrate model systems[16–18,23,24]. This model proposes that β-catenin is recruited to the DC through a conserved binding motif (βcatBM) on Axin and one or more β-catenin binding sites on APC[17,24,25] (Fig. 1B,C). Recruitment of β-catenin to the DC mediates sequential phosphorylation of its degron by CK-1α and GSK-3β leading to its ubiquitylation and proteasome-mediated degradation[17,24–26]. Current models postulate that following β-catenin phosphorylation on Axin, one of the 20 amino acid repeats on APC becomes phosphorylated and then phosphorylated β-catenin is moved to this APC domain prior to being transferred to the proteasome[16,27].

While the cWnt pathway is deeply conserved with homologs of most major components of the basic pathway found in all metazoan phyla[1,6,7,28], ongoing genomic sequencing studies in early branching metazoan clades have raised interesting fundamental questions about the origin and regulation of the Wnt signaling pathways. There are four extant clades of "pre-bilaterians" – ctenophores, sponges, placozoans, and cnidarians (Fig. 1B). Structure-function studies on how the DC is regulated have not been done in any of these four taxa. However, the emerging knowledge of cWnt pathway function in cnidarians (e.g., sea anemones, corals, "jelly fish"), the closest outgroup to the Bilateria (Fig. 1B), provides the best experimental systems to functionally understand the direction of evolutionary change in the cWnt signaling pathway[13,29–33].

One of the first observations that raised the possibility that the non-bilaterian cWnt DC may not function like the bilaterian DC came from a phylogenetic analysis of Wnt pathway components in two early emerging taxa, the poriferan *Amphimedon queenslandica* and the cnidarian *Nematostella vectensis*[6,34]. This work showed

substantial differences in known domain structure in DC components between these species and bilaterians. For example, the Axin proteins from *A. queenslandica* and *N. vectensis* appeared to lack the highly conserved βcatBM seen in bilaterian Axin that mediates its interaction with β-catenin[6,34] (Fig. 1B). We have confirmed that Axin from a ctenophore and a placozoan also lack this domain (Fig. 1B). Additionally, APC in these taxa were significantly shorter than the bilaterian homologs and lacked many of the critical protein-protein interaction domains seen in bilaterians[6,34] (Fig. 1C) and these genes have recently been classified as APC-like[35]. Adamska et al. (2010)[34] suggested that the Axin and APC-like proteins in these early diverging taxa may not be part of the DC, or that these proteins may be interacting in novel ways to regulate DC function. These observations provide a fundamental opportunity to better understand the evolution of a major metazoan signaling pathway and its potential role in animal diversification.

To investigate how cWnt DC could function without critical conserved domains identified in bilaterians we used functional molecular approaches combined with new bioinformatics tools to interrogate if Axin and APC-like had an active. cWnt DC function in embryos of the cnidarian model *Nematostella*. We demonstrate that even in the absence of the conserved bilaterian βcatBM the *Nematostella* Axin protein can robustly regulate cWnt signaling in *Nematostella* and in a bilaterian (sea urchin) embryo. AlphaFold[36–38] predictions and *in vitro* protein-protein interaction assays revealed that Nvβ-catenin interacts relatively weakly with NvAxin but binds strongly to NvGSK-3β. Moreover, we show that NvAPC-like protein binds to Nvβ-catenin and interacts with NvAxin, despite NvAPC-like lacking the protein-protein interaction domains mediating these interactions in bilaterian APC. Using AlphaFold to predict

potential NvAxin and Nvβ-catenin binding interfaces, we discovered an amino acid sequence on NvAxin that has similarity to the bilaterian βcatBM, but this sequence is embedded in the RGS domain at the amino-terminus rather than between the GID and DAX domains as seen in bilaterian Axin (Fig. 1B). We also used Alpha Fold to show that similar sequences are also present in poriferan and ctenophore Axin-RGS, but not in the bilaterian Axin-RGS. In summary, this first functional study of the regulation of a non-bilaterian DC function shows significant differences from regulation of the bilaterian cWnt DC and provides novel insight into the stepwise evolution of critical domains involved in regulatory modules in metazoan signal transduction pathways.

Results

Critical domains required for DC function in bilaterian Axin and APC are missing in non-bilaterian homologs

Structure-function studies in bilaterians have defined highly conserved regions on the Axin and APC proteins that mediate their interactions between each other, with β-catenin, and other proteins critical for regulation of cWnt signaling[17,19–24], (Fig 1B,C). Bioinformatic analyses showed that the critically conserved β-catenin-binding motif is absent in Axin proteins from all four non-bilaterian taxa[34] (Fig. 1B; Supplementary Table 1). Our bioinformatic analysis also corroborated the previous observations of Adamska et al.[34] who reported that the well-defined domains on APC that mediate its binding to β-catenin and ability to heterodimerize with Axin are missing in the cnidarian *Nematostella* and the sponge *Amphimedon* (Fig 1C). We could not recover an APC-like sequence in the ctenophore *Mnemiopsis* and the available APC-like sequence for the placozoan *Trichoplax* is incomplete. These observations raised the possibility

that non-bilaterian Axin and APC-like would not be able to interact with β-catenin and moreover, that in the absence of the SAMP domains (Fig. 1C), APC-like would not be able to heterodimerize with Axin to regulate β-catenin stability.

NvAxin regulates cWnt signaling in Nematostella embryos

We have previously shown that a bilaterian Axin protein can disrupt early development in *Nematostella*[29]. But to the best of our knowledge, heretofore a functional role for a non-bilaterian Axin in regulating cWnt signaling has not been examined in any non-bilaterian species. Whole mount in situ hybridization (WMISH) analysis of Axin expression showed broad expression in unfertilized eggs through the blastula stage and expression at the oral pole at the gastrula through the planula stages (Supplementary Fig. 1). We next asked if disrupting *NvAxin* function affected cWnt signaling during early *Nematostella* development. It is now well established that cWnt signaling regulates cell fates along the oral-aboral axis in *Nematostella*[3,13,39–41], and blocking β-catenin nuclear signaling using a dominant-negative form of NvTcf leads to the disruption of normal gastrulation and downregulation of genes in cell types derived from animal-half blastomeres, the endomesoderm and pharynx[39] (Supplementary Fig. 2). To determine if NvAxin regulates cWnt signaling and the nuclearization of β-catenin in embryos, we co-expressed NvAxin-GFP with Nvβ-catenin-mCherry by mRNA injection into zygotes and examined developing embryos for Nvβ-catenin-mCherry expression at the blastula stage. Our results showed that while control embryos co-injected with *GFP* and *Nvβ-catenin-mCherry* mRNA exhibited nuclearization of Nvβ-catenin-mCherry protein on one side of the embryo, embryos co-expressing either NvAxin-GFP or SpAxin-GFP and Nvβ-catenin-mCherry did not display any nuclear

localization of Nvβ-catenin-mCherry (Fig. 2A-C). This result indicated that NvAxin could block nuclearization of Nvβ-catenin, presumably through an active DC.

Earlier studies had demonstrated that blocking cWnt signaling by manipulating several different components of the pathway all produced a similar phenotype in *Nematostella* embryos[13,29,39]. These studies noted that while the embryos in which cWnt was downregulated underwent primary invagination and formed an endodermal epithelium, this epithelium failed to express endomesodermal markers and began to disintegrate by the late gastrula stage[29,39]. Consistent with these previous observations, overexpression of NvAxin produced embryos that underwent primary archenteron invagination but embryos failed to maintain a normal endodermal epithelium compared to controls[29,39] (Fig. 2D-F).

We next investigated if manipulating Axin levels in *Nematostella* embryos had an effect on endogenous gene expression consistent with a function for NvAxin in the cWnt DC. We reasoned that overexpressing NvAxin would lead to a downregulation of cWnt-dependent gene expression[39], while downregulation of NvAxin would lead to an increased expression of these genes. Consistent with these predictions, overexpression of NvAxin- or sea urchin (*Strongylocentrotus purpuratus)* Axin (SpAxin) in *Nematostella* embryos by mRNA injection into zygotes led to downregulation of genes expressed in the central-domain and central-ring syn-expression domains (Fig. 2G) compared to control embryos[39] (Fig 2G,H,I). To determine the effect of downregulating NvAxin expression on *Nematostella* development we knocked out the gene using CRISPR/Cas9, and examination of these animals when control polyps were at the four-tentacle stage, showed that the Axin-knockout polyps had supernumerary tentacles (Fig. 3Aa,Ab,Ac). This phenotype is consistent with the result observed when NvAPC-like

was knocked out in a previous study[30] which we also saw when we knocked out NvAPC-like using CRISPR/Cas9 (Figure 3Aa,Ab,Ac). Animals injected with *NvAxin* plus *NvAPC-like* gRNA with Cas9 typically showed a more severe phenotype with additional ectopic tentacles present throughout the animal (Fig. 3Ad). The NvAxin gRNA-mediated genome editing was validated by sequencing around the NvAxin gRNA excise sites in four single NvAxin gRNA-injected embryos and one Cas9-injected embryo (Supplementary Fig. 3) and by using WMISH to detect *NvAxin* expression in embryos at 24 hpf compared to controls (Fig. 3B). The percentage of successful excisions using CRISPR/Cas9 in this study is consistent with other studies that have used this method for gene editing in *Nematostella* (Fig. 3B)[30,42]. QPCR analysis revealed that the genes expressed in the central-domain and central-ring were all upregulated in *NvAxin* and *NvAPC-like* knockout embryos indicating that knockout of these two genes led to increased cWnt signaling consistent with a function for NvAxin and NvAPC-like in the cWnt DC (Fig. 3C,D). The morphological and molecular phenotypes seen with CRISPR/Cas9-mediated NvAxin and NvAPC-like knockout were phenocopied when NvAxin and NvAPC were knocked-down using antisense-morpholinos (Supplemental Fig. 4). It is important to note that the phenotypes generated by knocking out or knocking down NvAxin and NvAPC-like are distinct from the phenotypes generated from overexpressing a stable ("active") form of β-catenin in *Nematostella* embryos[39]. It is likely that there are maternal pools of NvAxin and NvAPC protein that are not affected by the CRISPR/Cas9 knockout or morpholino-mediated knockdown and the phenotypes that we observed are most likely due to disruption of cWnt during oral-aboral axis patterning rather than on specification of the endomesoderm by nuclear β-catenin[3,39,40]. Nevertheless, these results provided evidence that Axin and APC play crucial roles in

negatively regulating cWnt signaling in *Nematostella* embryos even though these proteins lacked domains essential for DC activity in bilaterians.

Nematostella Axin overexpression disrupts cWnt signaling in embryos of the sea urchin Strongylocentrotus purpuratus

We next sought to determine if *Nematostella* Axin could regulate cWnt signaling in a bilaterian. Extensive work done in sea urchin embryos has shown that β-catenin is nuclearized in vegetal blastomeres during early cleavage stages and blocking this nuclearization produces a distinct anteriorized phenotype[43–45]. When *S. purpuratus* (Sp) β-catenin-mCherry was expressed in sea urchin embryos by mRNA injection into zygotes, live imaging showed typical nuclearization of Spβ-catenin-mCherry at the vegetal pole[43,45] (Fig. 4Aa). However, when Spβ-catenin-mCherry was co-expressed with NvAxin or SpAxin there was complete elimination of this nuclearization (Fig. 4Ab,Ac). Moreover, consistent with previous observations where blocking β-catenin nuclearization by SpAxin-overexpression led to severe anteriorization of sea urchin embryos compared to control embryos[43] (Fig. 4Ba,Bb), overexpression of NvAxin in sea urchin embryos also led to a phenotype indistinguishable from the irreversible anteriorized phenotype produced by SpAxin-overexpression (Fig. 4Bc, 4Ba'-c'). Consistent with the anteriorized phenotype, analysis of gene expression in sea urchin embryos overexpressing NvAxin or SpAxin showed that endomesoderm gene markers were significantly downregulated, while two neuroectoderm gene markers were upregulated (Fig. 4C,D). These results clearly demonstrate that NvAxin is a strong regulator of cWnt signaling in a bilaterian, even though it lacks the conserved bilaterian βcatBM.

The NvAxin GSK-3β interacting domain (GID) is required for its function in the cWnt pathway

In bilaterians, the βcatBM on Axin is critical for the protein to function in the DC[17,21,25,27]. NvAxin lacks this domain, but it has the APC- (RGS), GSK- (GID), and Dvl- (DAX) binding/interacting domains, which are also found in the Axin proteins of the other non-bilaterians (Fig. 1B). Since our studies showed that NvAxin could regulate cWnt signaling in the sea urchin embryo, we used a rescue assay that we had previously developed to study Axin structure/function in sea urchins[43] to identify the domains on NvAxin required for β-catenin regulation. This rescue assay takes advantage of the unique "posteriorized" phenotype produced in sea urchin embryos when levels of Axin in the embryo are reduced using an Axin morpholino that results in ectopic β-catenin nuclearization. This phenotype can be rescued by overexpressing the wildtype Axin protein[43] (Fig. 5A-C). When we co-injected the Axin morpholino with full-length *NvAxin* mRNA or *GFP* mRNA into zygotes and analyzed developing embryos we noted that while the embryos co-injected with the Axin morpholino and *GFP* mRNA were posteriorized as expected (Fig. 5Ca,a'), the embryos co-injected with the Axin morpholino and *NvAxin* mRNA were completely rescued (Fig. 5Cb,b'). Similarly, co-injection of the Axin morpholino with *NvAxinΔRGS* mRNA or *NvAxinΔDAX* mRNA efficiently rescued the Axin morpholino-induced posteriorized phenotype (Fig. 5Cc-d'). However, co-injection of the Axin MO with *NvAxinΔGID* mRNA failed to rescue the phenotype (Fig. 5Ce,e'), indicating the requirement of the GID for NvAxin to function in the cWnt DC. We conclude that in *Nematostella*, the Axin GSK-3β-interacting domain

is likely the most crucial NvAxin domain for regulating β-catenin stability in the cWnt DC.

Previous studies in bilaterians have shown that overexpression of the Axin-GID alone is sufficient to activate cWnt signaling[46]. The mechanism for this is still unclear but it has been suggested that the GID can bind to endogenous GSK-3β and prevent it from interacting with Axin[46–48]. Our NvAxin rescue experiments in sea urchins using Axin domain deletion constructs clearly showed that the GID is required for NvAxin's activity in the cWnt DC (Fig. 5). GSK-3β binding to Axin is a critical step in assembling the DC in bilaterians[17,27]. To begin to assess if the NvAxin-GID was involved in regulating GSK-3β in *Nematostella* we first overexpressed an NvGID-GFP construct in embryos by microinjection of mRNA into zygotes. When control animals were at the polyp stage, the NvGID-GFP overexpressing embryos had a morphology resembling *Nematostella* embryos overexpressing an activated form of β-catenin[39] (Fig. 6A). Analysis of germ layer-specific markers at the blastula stage using qPCR showed that all endomesoderm gene markers and pharyngeal markers were highly upregulated as expected while the ectoderm gene markers were downregulated (Fig. 6B).

The residues within the Axin-GID required for interactions with GSK-3β are highly conserved in bilaterians and all four non-bilaterian taxa[47] (Supplementary Fig. 5). This conservation suggested that the phenotype elicited by overexpression of NvAxin-GID in *Nematostella* was due to it directly binding to NvGSK-3β and preventing NvGSK-3β from binding to NvAxin. To determine if the NvAxin-GID could directly interact with NvGSK-3β, we mixed NvAxin-GID-GFP and NvGSK-3β-mCherry proteins made using *in vitro* transcription and translation (TnT) and immunoprecipitated (IP) NvAxin-GID-GFP using anti-GFP antibodies. Western blot analysis of the IP samples

using anti-mCherry antibodies showed a direct interaction between NvAxin-GID-GFP and NvGSK-3β-mCherry *in vitro* (Fig. 6C). In summary, these results are consistent with the notion that NvAxin scaffolds a critical DC component, GSK-3β, similar to bilaterian Axin function in the DC.

NvAxin lacks the conserved β-catenin binding motif, but can interact weakly with Nvβ-catenin in vitro and in vivo

Previous studies in bilaterian taxa such as vertebrates and dipterans have shown strong interactions between Axin-APC, Axin-β-catenin, APC-β-catenin, and Axin-GSK-3β *in vitro* and *in vivo*[16,21,23,24,47,49,50]. In addition, these studies have documented that while there is a single defined β-catenin binding motif on bilaterian Axin, there are multiple β-catenin binding domains on APC that have distinct sequence motifs[16,18,23,51] (Fig. 1C). The lack of a recognizable β-catenin-binding domain on all the non-bilaterian Axin proteins we examined raised the question whether these proteins could still interact with β-catenin possibly through binding domains previously uncharacterized in bilaterians. To explore this possibility, we first used AlphaFold[36–38] to predict potential protein-protein interactions between various protein pairs. This analysis identified potential interactions between SpAxin-Spβ-catenin and SpAxin-SpGSK-3β based on complementary domains seen in orthologs from other bilaterian proteins (Supplementary Fig. 6A,B). Moreover, as predicted from the conserved domains, AlphaFold also predicted an interaction between NvAxin and NvGSK-3β (Supplementary Fig. 6C). Based on iPTM and PTM values, interactions between NvAxin-Nvβ-catenin and NvAPC-like-Nvβ-catenin were also predicted (Supplementary Fig. 5D,E). In contrast, interactions between NvAxin-NvAPC-like and NvAPC-like-

NvGSK-3β were not supported by AlphaFold analysis (Supplementary Fig. 6F,G). To experimentally validate the predicted direct protein-protein interactions we mixed the *in vitro* synthesized protein pairs and carried out IP followed by Western blot analysis. This assay revealed an expected robust interaction between SpAxin-GFP and Spβ-catenin-mCherry (Fig. 7A, Lane 5). We also noted a weaker but consistent interaction between NvAxin and Nvβ-catenin and NvAxin and Spβ-catenin proteins in vitro (Fig. 7A, Lane 1,2).

We next asked if sea urchin Axin could interact with Nvβ-catenin. To our surprise, despite SpAxin containing a conserved βcatBM (Fig. 1B) and a demonstrated ability to strongly interact with Spβ-catenin in vitro, it only displayed a relatively weak interaction with Nvβ-catenin in this assay (Compare Fig. 7A, Lane 4 and Lane 5). These results suggested that the Axin-interacting armadillo (ARM) repeat domains on Nvβ-catenin have diverged from the corresponding domains on bilaterian β-catenin, and hence it was unable to interact strongly with a bilaterian Axin. *Nematostella* β-catenin has all 12 ARM domains seen in bilaterians and each ARM repeat in Nvβ-catenin forms a group with corresponding ARM domains in bilaterian β-catenin indicating a high degree of conservation over 700 million years of evolution[15]. Hence, any changes in Nvβ-catenin protein that affects how it interacts with a bilaterian Axin βcatBM would likely be subtle amino acid changes that affects binding-affinity between the proteins. We conclude that NvAxin can interact with *Nematostella* and sea urchin β-catenin, but based on the *in vitro* assay, these interactions appeared considerably weaker than the interaction between SpAxin and Spβ-catenin.

We next asked if NvAxin could interact with NvGSK-3β in the *in vitro* pull-down assay. As predicted by the presence of a conserved GID on NvAxin and our previous

observation that the NvAxin-GID can interact with NvGSK-3β, Western blotting of the IP products showed a clear interaction between NvAxin-GFP and NvGSK-3β-mCherry as did SpAxin-GFP and SpGSK-3β-mCherry (Fig.7A, Lane 3, 6).

In bilaterians, Axin and APC proteins heterodimerize to form the principal scaffold for the β-catenin DC and the APC SAMP domains are required for this interaction[23,24] (Fig 1C). NvAPC-like is significantly smaller in size than bilaterian APC, and when we analyzed its domain structure we noted that it had the conserved armadillo repeats, one poorly characterized repeat region predicted to interact with Axin, and another uncharacterized repeat region at the amino-terminus of the protein, but did not have the SAMP domains (Fig 1C). To determine if NvAPC-like could yet potentially directly interact with NvAxin, Nvβ-catenin or NvGSK, we mixed NvAPC-like-mCherry in vitro with NvAxin-GFP, Nvβ-catenin-GFP or NvGSK-3β-GFP followed by IP and Western blots analysis using anti-mCherry antibodies. We noted that NvAPC-like robustly interacts with Nvβ-catenin in this assay (Fig. 7B). This interaction is also predicted by AlphaFold (Supplementary Fig. 6H). We were also able to detect interactions between NvAPC-like and NvGSK-3β and NvAPC-like and NvAxin in vitro (Fig. 7B). AlphaFold also predicted a strong interaction between one of the repeat regions of NvAPC-like and the NvAxin RGS domain (Supplementary Fig. 6I) suggesting that this may be the potential mechanism for NvAPC-like-NvAxin heterodimerization (Fig 7B).

The *in vitro* assay that we used in the experiments described above provides insight into potential direct interactions between components of the cWnt DC in *Nematostella* embryos. However, in those cases where we failed to detect any direct interactions or saw weak interactions *in vitro*, it is possible that in the *in vivo*

environment, post-translational modifications or bridging proteins in the embryo might promote protein-protein interactions, or higher-affinity interactions[23,24,27,52]. To test this idea we tagged Axin and β-catenin proteins from *Nematostella* and the sea urchin *S. purpuratus* with the split Click Beetle Green (CBG) luciferase system[53] (Supplementary Fig.7) and possible pairs of Axin and β-catenin proteins were expressed in *Nematostella* embryos by mRNA injection into zygotes and the signals were quantified *in vivo* and in embryo lysates (Supplementary Fig. 7). Consistent with the *in vitro* studies, SpAxin + Spβ-catenin had the highest signal in both embryonic lysates and live embryos, while NvAxin + Spβ-catenin showed a relatively lower signal (Supplemental Fig. 7A,B). Moreover, the *in vivo* and *ex vivo* experiments confirmed that NvAxin and Nvβ-catenin, and SpAxin and Nvβ-catenin are only capable of relatively weak interactions most likely discounting any *in vivo* enhancement of these interactions.

We next addressed the molecular basis for the persistent, albeit weak, *in vitro* and *in vivo* interactions we noted between NvAxin and Nvβ-catenin (Fig. 7A; Supplemental Fig. 7). Using AlphaFold3, we identified a possible region of interaction for Nvβ-catenin with NvAxin in a sequence located within the NvAxin-RGS domain (Fig. 8A; Supplementary Fig. 8A,A',D). Alignment of the predicted NvAxin β-catenin interaction site with the conserved bilaterian β-catBM using Clustal Omega and Jalview showed some amino acids to be highly conserved between these sequences (Supplementary Fig. 8D). Significantly, the conserved leucine at position 119 in NvAxin corresponds to a residue known to be essential for the interaction between bilaterian Axin and β-catenin[47] (Supplementary Fig. 8D). Additionally, the histidine at position 504 in *Drosophila* Axin has been shown to be critical for β-catenin interaction with Axin[47]. In the sequence in *Nematostella* Axin-RGS, this corresponding residue is

missing, possibly accounting for the weak interaction between NvAxin and Nvβ-catenin (Supplemental Fig. 8D). Additional AlphaFold analysis of potential Axin and β-catenin interaction in the ctenophore *M. leidyi* and the poriferan *A. queenslandica* also predicted interactions between β-catenin and a sequence similar to βcatBM also located within the Axin-RGS domain (Fig. 8A; Supplementary Fig. 8E,F). Alignment between the predicted MlAxin β-catenin binding site and the bilaterian β-catBM did not reveal conservation of the leucine residue; instead, an aspartic acid was identified (Supplementary Fig. 8E). However, the putative sponge AqAxin β-catenin binding site retained the conserved leucine associated with functional binding (Supplementary Fig. 8F). We used AlphaFold to determine if there were any putative β-catenin interaction motifs on the Axin-RGS domains of mouse and *Drosophila* but were not able to detect any sequence that matched the sequences we found embedded in the Axin-RGS domains of *Nematostella*, *A. queenslandica* and *M. leidyi* Axin proteins (not shown).

Discussion

In this study we functionally characterized the regulation of the cWnt DC in the cnidarian *Nematostella*. We show that *Nematostella* has a robust DC to control β-catenin stability, but our results show that this DC is regulated differently in comparison to the bilaterian DC. In addition, our results provide novel insight into what the ancestral DC may have looked like in the cnidarian-bilaterian last common ancestor (LCA).

The cWnt destruction complex in *Nematostella* functions differently than the bilaterian DC

Current models propose that in the bilaterian DC, β-catenin has to bind to both Axin and APC and that these proteins need to heterodimerize for efficient regulation of DC function[8,16,18,24,27]. But Axin and APC-like in cnidarians and other non-bilaterians lack the domains required for these interactions. Our *in vitro* and *in vivo* experiments showed that while NvAxin binds Nvβ-catenin relatively weakly it binds robustly to NvGSK-3β, and NvAPC-like binds robustly to Nvβ-catenin. Moreover, our *in vitro* experiments showed that NvAxin and NvAPC-like can interact directly and *in vivo* this interaction would likely bring β-catenin and GSK-3β together for phosphorylation of the β-catenin degron. In our efforts to identify NvAxin sequences underlying the weak but consistent interaction between NvAxin and Nvβ-catenin using AlphaFold we identified a sequence with a high degree of similarity to the conserved bilaterian βcatBM but this sequence was embedded within the NvAxin-RGS domain (Fig. 8A; Supplementary Fig. 8). Similar sequences were found embedded in the Axin-RGS domains of *A. queenslandica* and *M. leidyi*, but not in bilaterian Axin-RGS (Fig. 8A; Supplementary Fig. 8). Within this sequence both NvAxin and AqAxin have a conserved leucine residue seen in the conserved β-catenin-binding motif in bilaterian Axin that has been shown to be critical for interaction between Axin and β-catenin in *Drosophila*[47] (Fig. 8A; Supplementary Fig. 8D,F). But this region of NvAxin and AqAxin lacked a highly conserved histidine that had also been shown to be critical for *Drosophila* Axin-β-catenin interactions[47] (Supplementary Fig. 8D,F). Our analysis showed that the putative β-catenin-binding motif in the *Mnemiopsis* Axin-RGS lacked the conserved leucine and histidine residues required for interaction of the bilaterian βcatBM with β-catenin (Supplementary Fig. 8E). It is now established that ctenophores are the earliest emerging metazoan taxon[54,55]. Hence, the phylogeny would predict that the putative

ancestral β-catenin-binding sequence likely acquired the leucine residue prior to the split of the poriferans from a LCA to placozoans, cnidarians and bilaterians, and bilaterian Axin acquired the critical histidine residue after splitting from a LCA with cnidarians. While we have not yet experimentally tested if this site on NvAxin-RGS mediates the weak interaction we see between NvAxin and Nvβ-catenin, our observations suggest a stepwise evolution of the β-catenin-binding site seen in bilaterian Axin. The position of the putative β-catenin-binding sequence in non-bilaterian Axin proteins suggests that the evolution of the β-catBM in bilaterians may have involved significant domain rearrangement within the Axin protein. In non-bilaterian species such as *Nematostella*, *Mnemiopsis*, and *Amphimedon*, the potential low-affinity β-catenin binding sequence is located within the Axin-RGS domain, and this contrasts with the positioning of the β-catBM in bilaterians, where it is located between the GID and DAX domains of Axin (Fig. 8B). This transition likely involved the translocation of the ancestral β-catenin binding sequence from the Axin-RGS domain to a more C-terminal location where it acquired relatively high-affinity β-catenin binding activity thereby supporting Axin's role as a scaffold in the destruction complex (Fig. 8B).

While our work showed that NvAPC-like-like can interact with β-catenin and form a complex with NvAxin and NvGSK-3β, other structural features of NvAPC-like indicated additional differences between the *Nematostella* and bilaterian cWnt DCs. Previous work has shown a clear role for NvAPC-like in regulating cWnt signaling in *Nematostella* and our results corroborated that work[30]. However, the structure of NvAPC-like predicts that this protein would not be able to carry out some critical roles in the DC attributed to bilaterian APC. For example, APC proteins from *Drosophila* and vertebrates have several 15 and 20 amino acid repeats that can bind to β-catenin and in

addition, these proteins have 2-3 SAMP domains that are involved in interactions with Axin[16,23,56,57] (Fig. 1C). The second 20aa repeat and an adjacent B sequence are particularly significant because current models propose that these domains are critical for phosphorylated β-catenin to be transferred from Axin to APC prior to being moved to the proteasome for degradation[16,23]. Strikingly, the NvAPC-like protein lacks any detectable 15aa and 20aa repeats or the SAMP domains but has seven predicted ARM repeats and two poorly characterized repeat regions (Fig. 1C). Hence, it appears that NvAPC-like resembles a severely truncated bilaterian APC protein, and one that would not be predicted to regulate β-catenin degradation in these systems[57]. What is striking from these observations is that the *Nematostella* DC can tightly regulate β-catenin signaling in *Nematostella* embryos even though NvAxin does not have the highly conserved βcatBM seen in bilaterians and NvAPC-like lacks the well-characterized β-catenin-binding domains that function to transfer β-catenin from Axin to the proteasome[16,23,24,51]. For example, when β-catenin is expressed in *Nematostella* embryos by mRNA injection the protein is initially broadly expressed, but then it is cleared from the vegetal pole blastomeres of the embryos and very tightly restricted to nuclei of the animal pole blastomeres[3,13,29,39]. This raises the question as to whether NvAPC-like has a role in shuttling phosphorylated β-catenin to the proteasome, or if cnidarians have a different mechanism to carry out this critical function. Future work will address this question and other intriguing questions raised by this work.

Evolution of the bilaterian cWnt destruction complex

We propose that the ancestral DC that was present in the LCA of Bilateria and Cnidaria was scaffolded by an APC-like protein that bound β-catenin and Axin and an

Axin protein that bound GSK-3β and had a "weak" β-catenin-binding site embedded in the Axin-RGS domain. The low-affinity β-catenin-binding site on Axin-RGS had the critical leucine residue that is conserved between the bilaterian βcatBM and the putative β-catenin-interacting sequence we identified in *Nematostella* using AlphaFold (Fig 8A; Supplemental Fig. 8D). This DC was capable of regulating β-catenin stability in the cWnt pathway in early emerging metazoans. Whether this DC was able to directly target β-catenin for degradation through the proteasome is not known at this time. Over time the low-affinity β-catenin-binding site was translocated to a position between the GID and DAX domains of bilaterian Axin and mutations in this sequence increased its affinity for β-catenin possibly by gaining the conserved histidine residue seen in the bilaterian βcatBM[47]. Likely in parallel, APC-like gained a long carboxy-terminal region that led to the acquisition of redundant β-catenin and Axin-binding sites. The overall consequence of these changes may have been a more efficient regulation of the DC and an increased level of redundancy that served to buffer this critical regulatory module from misregulation[16,50] (Fig. 8B). This idea is consistent with modeling studies which have shown that signaling pathways evolve increased levels of complexity under standard evolutionary conditions, and this complexity also provides increased robustness[58]. It is also likely that the increased number of interfaces provided by the bilaterian Axin and APC proteins provided additional targets for context-dependent regulation of the cWnt DC during the evolution of complex body plans in the Bilateria. The approach that we have taken in this study opens up opportunities to carry out additional structure-function studies in non-bilaterians to examine the evolution of signal transduction pathways.

Materials and Methods

Animal care, spawning and culture

Adult *N. vectensis* were spawned and eggs prepared for microinjections as previously described[41].

Adult *Lytechinus variegatus* (Lv) sea urchins were obtained from Duke University Marine Lab (Beaufort, NC) or Pelagic Corporation (Sugarloaf Key, FL). Spawning of animals and collection and treatments of gametes was done as previously described[43].

Cloning full length NvAxin and Reverse Transcriptase-PCR analysis

Full length *N. vectensis* Axin (NvAxin) cDNA was PCR-amplified from egg stage using primers designed against the NvAxin sequence (NEMVEDRAFT_v1g182113). The primer sequences were: NvAxin FL forward primer: CGCGCGGATCCATGAGCGAAGAGTTGTGTAG, and NvAxin FL reverse primer: CGACCATCGATTGAGTCTACTTTTTCTACTTTGC. Egg, cleavage, blastula, gastrula and planula stage embryos were collected separately for RNA extraction using Trizol reagent (cat# 15596026, Invitrogen). Approximately 1 µg of total RNA was used for cDNA synthesis using SuperScript IV first strand synthesis system (cat# 18091200, Invitrogen). For PCR, NvAxin cDNA was amplified from different stage embryos. The primers used to amplify NvAxin for RT-PCR were: NvAxin FP: ATGAGCGAAGAGTTGTGTAG, and NvAxin RP: CGTGCATCTTGCTCGTCGTG.

The PCR procedures followed the protocol provided with the Q5 high fidelity DNA polymerase kit (cat# M0491, NEB) with thermal cycling conditions, 98°C for 30 seconds, 35 cycles with (98°C 10 seconds, 62°C 30 seconds, 72°C 20-30 seconds/kb)

and 72°C for 2 minutes. The wildtype NvAxin was inserted into the GFP-pCS2^{+} vector by BamH1 and Cla1 restriction enzyme digestion and ligation with T4 DNA ligase.

Making NvAxin domain deletion constructs by site-directed mutagenesis

NvAxinΔRGS, NvAxinΔGID, NvAxinΔDAX constructs were made using the Q5 Site-directed mutagenesis kit (E0554, NEB). Primers were designed to delete the RGS, GID and DAX domains separately. The following primer sequences were used: NvAxin ΔRGS forward primer, CAGGCTCACAGAGACACC, and NvAxin ΔRGS reverse primer, GAGTTAGCCCATCGCTCG; NvAxin ΔGID forward primer, TGAGAGTGAATATGGCCAG, and NvAxin ΔGID reverse primer, GGATTTTTGGCTTCCTTTG; NvAxinΔDAX forward primer, CAATCGATTCGAATTCAAG, and NvAxinΔDAX reverse primer, TTGTGTTTCTCCTTTTTCC. To perform the PCR procedure, the NvAxin-GFP pCS2+ plasmid was mixed with pairs of primers, the Q5 hot start high-fidelity 2X master mix and nuclease free water to perform PCR procedure, followed by kinase, ligase & Dpnl (KLD) treatment.

Microinjection of morpholino antisense oligonucleotides and mRNAs

For knockdown experiments, morpholino antisense oligonucleotides to Axin or APC-like (NvAxin MO or NvAPC MO) and a standard control morpholino (Control MO) to a random nucleotide sequence (5'-CCTCTTACCTCAGTTACAATTTATA-3') were synthesized at Gene Tools, LLC (Eugene, OR). The NvAxin MO: TACACAACTCTTCGCTCATCTCACG or NvAPC-like MO: ATCCTCTTCAAAATCGTCCATGTTG were designed to span the start codon of the Axin

or APC-like transcripts. Each MO was injected at a final concentration of 2 mM in 30-40% glycerol and dextran rhodamine 0.2 μg/μl (D1824, Invitrogen).

For overexpression experiments in *N. vectensis* or *L. variegatus*, the NvAxin-GFP, NvAxin ΔRGS-GFP, NvAxin ΔGID-GFP, NvAxin ΔDIX-GFP, SpAxin-GFP, Nvβ-catenin-mCherry, and Spβ-catenin-mCherry, NvAxin GID-GFP, and a control GFP mRNA were all cloned into the pCS2+ vector. The pCS2+ vectors containing the respective cDNAs were linearized with NotI and mRNA was transcribed using the SP6 mMessage mMachine Kit (Ambion® ThermoFisher Scientific). The dominant-negative NvTcf (NvdnTCF) construct[39] was used for downregulating cWNT signaling. This construct was in the Venus-pDEST expression vector. The dnTCF-Venus construct was linearized with Acc65I and *in vitro* transcribed as previously described[39]. The mRNAs were mixed in 40% glycerol to a final concentration of 0.5 μg/μl. *GFP* mRNA was overexpressed as a control at the same molar ratio as previously described[59].

For co-overexpression experiments in *N. vectensis* or *L. variegatus*, *NvAxin-GFP*, *NvAxin ΔGID-GFP*, *SpAxin-GFP*, *Nvβ-catenin-mCherry*, *Spβ-catenin-mCherry* mRNAs were injected at a final concentration of 0.5 μg/μl, 0.5 μg/μl, 0.5 μg/μl, 0.2 μg/μl, 0.2 μg/μl respectively in 40% glycerol.

For each experiment, more than 100 embryos were injected per MO or per mRNA. The experiments were repeated at least three times for biological replication.

CRISPR/Cas9 mediated knockouts and microinjections

To knock out *NvAxin* or *NvAPC-lik*e, the synthetic guide RNAs (sgRNA; Synthego, Inc.) and Cas9 complex (RNP complex) were introduced into *N. vectensis* embryos by microinjection into zygotes. The *NvAxin* or *NvAPC-like* single guide RNAs

were designed using CRISPRscan and CHOPCHOP as previously described[60]. Each single guide RNA was resuspended to 50 μM and stored at -80°C. Cas9 was obtained from PNA bio (Cat.# CP01). Cas9 was reconstituted to 5 mM and was aliquoted for single use and stored at -80°C.

A mixture (2.5 μl) containing sgRNA (12 μM), Cas9 (0.6mM), 40% Glycerol, dextran rhodamine (0.2 μg/μl) and nuclease free H_2O was prepared and 1 μl of mixture was loaded into needles for microinjection. The same amount of Cas9 only was injected as a control. *NvAxin* sgRNA was used to introduce mutations into *NvAxin*, and *NvAPC-like* sgRNA was used to introduce mutations into *NvAPC-like*, and the mixture of *NvAxin* and *NvAPC-like* sgRNAs were used to mutate both genes in single embryos.

Genomic DNA extraction from single embryos and validation of DNA editing by CRISPR/Cas9

Single *NvAxin* gRNA injected embryos were collected into 0.2 ml PCR tubes and lysed by adding 20 μl of extraction buffer for 100 μl buffer: 1 μl 1M Tris, pH8.0; 0.3 μl Tween 20; 0.2 μl 0.5M EDTA; 5 μl 1M KCl; 0.3 μl NP40; 2.5 μl proteinase K (20 mg/ml); nuclease free water). The tubes with lysed embryos were incubated for 3 hr at 55°C in a thermal cycler with periodic vortexing and the reaction was inactivated by heating the tubes at 98°C for 5min. For the PCR analysis of *NvAxin* gRNA injected embryos, 5 μl of genomic DNA was used as a template to carry out the PCR reaction as described above for NvAxin cloning and then the amplicon was gel extracted, purified and sequenced at Eurofins Scientific. The following primers were used to generate the NvAxin amplicons from genomic DNA from embryos edited with the *NvAxin* gRNA:

forward primer: ATGGCCAGTCTAAAAAGTCTATCC, and reverse primer: CTGGTGGTTCAATGTCAAGAACGGTAT.

Quantitative PCR (qPCR)

To evaluate the effects of injected gRNAs, MO or mRNA on lineage-specific gene expression, quantitative PCR (qPCR) was performed on *N. vectensis*, or *L. variegatus* cDNA samples synthesized from total RNA that was extracted from gRNA-, morpholino- or mRNA-injected embryos. The control and treated samples were collected at the blastula stage; *N. vectensis* embryos were at 24 hpf at 17°C and *L. variegatus* embryos were at 6 hpf at 25°C. Total RNA was isolated using the Trizol reagent solution (cat# AM9738, Invitrogen). The cDNA was synthesized from 50 -100 ng total RNA of control and experimental embryos respectively using the qScript cDNA Synthesis kit (Quanta Biosciences, Beverly). The PerfeCTa SYBR Green FastMix (Quanta Biosciences, Beverly) was used for assembling the qPCR reactions. Each experiment was repeated 3 times with separate batches of embryos and each PCR reaction was done in triplicate.

The expression of selected genes was analyzed using the delta delta Ct ($2^{-\Delta\Delta Ct}$) method as previously described[43]. All the *L. variegatus* primer sequences were obtained from David McClay's laboratory at Duke University.

Whole mount in situ hybridization (WMISH)

NvAxin expression during early development was determined using whole mount in situ hybridization (WMISH). The *NvAxin* in situ hybridization probe was made using a pair of primers specifically targeting NvAxin: NvAxin-F: 5' CGAAGGTAGAGCCGTATC 3', and NvAxin-R:

ATTTAGGTGACACTATAGGTCCGTCAGAGCATCACT, and was designed to contain a Sp6 promoter for *in vitro* RNA synthesis. Embryo fixation and WMISH were performed as previously described[41]. Embryos were fixed in 4% paraformaldehyde with 0.2% glutaraldehyde in PTw (1XPBS+ 0.1%Tween-20) for 2 min at room temperature, and then fixed in 4% paraformaldehyde in PTw for 1 hr at 4 °C. In each experiment, a final concentration of 1 ng/µL anti-sense *NvAxin* probe was used which was hybridized at 63°C for 2 days. *NvAxin* expression was detected using NBT/BCIP as a substrate for the alkaline phosphatase conjugated to anti-digoxigenin fab fragments (1:5000; Roche).

F-actin and nuclear staining

The morphology of *dnTcf-*, *NvAxin-*, *SpAxin-* and control *GFP*-RNA injected embryos was examined using embryos collected at late gastrula stage (48 hpf at room temperature) that were fixed and stained for F-actin and nuclear staining. Embryos were collected and fixed as previously described with modifications[13,29]. Briefly, embryos were first fixed in fix1 (100 mM HEPES pH 6.9; 0.05 M EGTA; 5 mM MgSO4; 200 mM NaCl; 1x PBS; 3.7% Formaldehyde; 0.2% Glutaraldehyde; 0.5% Triton X-100; and autoclaved ultrapure water) for 2-3 minutes and then fixed in fix2 (100 mM HEPES pH 6.9; 0.05 M EGTA; 5 mM MgSO4; 200 mM NaCl; 1x PBS; 3.7% Formaldehyde; 0.05% Glutaraldehyde; 0.5% Triton X-100; and autoclaved ultrapure water) for one hour at room temperature on the rocker. Fixed embryos were rinsed in PBT (X% Tween 20 in 1 x PBS, pH7.4) for 30 mins x 4 times. Embryos were blocked with 5% normal sheep in PBT buffer for 1 hour at room temperature on the rocker then rinsed with PBT for 30 mins x 4 times. For the F-actin staining, embryos were stained with Phalloidin in PBT for 1 hour and then rinsed with PBT for 10 min x 2 times. For nuclear

staining, embryos were incubated in DAPI in PBT for 1 hour, and then rinsed in 1xPBS (PH 7.4) for 10 min x 3 times. Following these washes, the embryos were dehydrated using a gradient of isopropanol (50, 75, 90, 100%, 100%). The embryos were then cleared with 1:2 benzyl benzoate: benzyl alcohol (BB:BA) for 1 min x 2 times and mounted in BB:BA for imaging using scanning confocal microscopy.

In vitro Transcription and Translation (TNT) and Western blot analysis

NvAxin-flag, Nvβ-catenin-mCherry, SpAxin-flag, Spβ-catenin-mCherry were in vitro transcribed and translated using the TnT® Quick Coupled Transcription/Translation System with SP6 RNA polymerase promoter (cat # L2080, Promega). Plasmids (at 2 μg each) containing the respective cDNAs coding for the various fusion proteins were incubated with TNT quick master mix at 30°C for 90 minutes. Protein expression was examined using Western blot analysis with anti-flag (cat# 740001) or anti-mCherry antibodies (PA5-34974) respectively. Approximately 5 μl of each protein was mixed with sample buffer (10% SDS, 500 mM DTT, 50% Glycerol, 250 mM Tris-HCL and 0.5% bromophenol blue dye, PH6.8) and denatured for 20 minutes at 60°C and loaded on an 8% SDS-PAGE gel. Protein gel was transferred onto Trans-Blot nitrocellulose membranes (Bio-Rad), the membranes were incubated with rabbit anti-mCherry antibody (1:1000) (PA5-34974, Invitrogen) or rabbit anti-flag antibody (1:1000) (cat# 740001, Invitrogen), and developed using goat anti rabbit IRDye 800 secondary antibodies (1: 10,000) (cat# C50331, LI-COR, Odyssey).

Protein-protein interactions were detected between the following four pairs of proteins, NvAxin-flag x Nvβ-catenin-mCherry; SpAxin- flag x Spβ-catenin-mCherry; NvAxin-flag x Spβ-catenin-mCherry; SpAxin- flag x Nvβ-catenin-mCherry using the

Pierce Crosslink Immunoprecipitation Kit with minor modifications (cat # 26147, Thermo Fisher Scientific, Waltham, MA). Forty µg of anti-flag antibody was used for the antibody resin column. Forty five µl each protein mix was raised to 500 µl with IP lysis/wash buffer and incubated with anti-flag coupled agarose resin overnight at 4°C for antigen immunoprecipitation and elution. All the steps were carried out on ice or 4°C unless otherwise indicated and all resin centrifugation steps were performed for 1 min at 1000 x g. Following the procedure 40 µl of each Co-IP elution was mixed with sample buffer and boiled for 5 minutes to denature proteins. Denatured protein samples were examined on an 8% SDS-PAGE gel followed by Western blot analysis. Protein gels were transferred onto Trans-Blot nitrocellulose membranes (Bio-Rad), the membranes were incubated with rabbit anti-mCherry antibody (1:1000) (PA5-34974, Invitrogen), and developed using goat anti rabbit IRDye 800 secondary antibodies (1:10,000) (cat# C50331, LI-COR, Odyssey).

Split luciferase assay

N- and C-terminal fragments of click beetle green (CBG) split luciferase, including polypeptide linkers, were amplified and blunt-end-ligated into pSPE3-RfA vectors in a single restriction-ligation reaction. Coding sequences for *N. vectensis* and S. *purpuratus* Axin and β-catenin were cloned into pENTR using D-TOPO cloning kit (Invitrogen K240020) and recombined into CBG-tagged destination vectors via Gateway cloning (Invitrogen 11791020). Nanoluciferase (NanoLuc) was similarly cloned and recombined into pSPE3-RfA.

Recombined Axin and β-catenin constructs were linearized, purified, and used for in vitro mRNA synthesis (Invitrogen AM1348). Equimolar CBG-tagged *Axin* and *β-*

catenin mRNA mixtures, along with NanoLuc mRNA and fluorescent dextran, were microinjected into *Nematostella* zygotes. At 28 hours post-fertilization(hpf), live embryos were collected, and luminescence was measured after adding D-luciferin substrate (Goldbio LUCNA-100). Embryos were then lysed with ONE-Glo EX Luciferase Assay Reagent (Promega N1610), and further measurements were taken. NanoDLR Stop & Glo Reagent (Promega N1610) was used to stop the CBG reaction and initiate NanoLuc luminescence. NanoLuc signal was used to normalize protein levels and CBG intensities. Average NanoLuc signal from 15-20 minutes after the addition of substrate was used to determine ratios of protein levels. Average relative intensities across timepoints were calculated for each construct combination.

Primers:

Name	Sequence
linker-N-luc Fw	CAGATCTCGTACGCGTCCC
N-luc Rev	TTAGCCGTCGTCGTCGAT
Kozak-CBG-C-linker Fw	CAGAAAAAATGAAGGGTTATGTCAATAACGTTG
C-luc-linker Rev	TCCGCCCCGGGACG
NvAxin Fw	CACCATGAGCGAAGAGTTGTGTAG
NvAxin Rev	TGAGTCTACTTTTTCTACTTTGC
NvBeta-catenin Fw	CACCATGGGGATGCAGCAGGG
NvBeta-catenin-STOP Rev	TCAGAGGTCTGTGTCATACAGAG
SpAxin Fw	CACCATGAGTCTAGAAGTGTATAGG
SpAxin Rev	GTGATCATCGACAGATTC
SpBeta-catenin Fw	CACCATGGAGCAGGCAAGGTAC
SpBeta-catenin-STOP Rev	TTACAGATCGGTATCAAAGAACG
NanoLuc Fw	CACCATGGTCTTCACACTCG
NanoLuc Rev	TTACGCCAGAATGCG

AlphaFold 3 Protein-Protein interaction prediction

Computational methods were used to predict protein-protein interactions among the components of the β-catenin destruction complex in *S. purpuratus* (sea urchin) and

Nematostella[36–38]. Protein sequences for the individual components of the β-catenin destruction complex were used as input in AlphaFold 3. The prediction accuracy was assessed using the predicted align error (PAE) and confidence scores such as the predicted TM-score (PTM) and inter-chain predicted TM-score (iPTM), which are indicators of the reliability of the predicted interactions. A PTM score above 0.5 indicates that the overall predicted fold for the complex may resemble the true structure. iPTM Values greater than 0.8 represent confident, high-quality predictions, while values below 0.5 suggest likely failed predictions. ipTM scores between 0.5 and 0.8 fall into an intermediate zone where predictions may be correct or incorrect[37]. AlphaFold 3 allowed for the visualization of possible binding interfaces and the determination of whether specific regions, such as the β-catenin binding domains, could facilitate protein-protein interactions, even in cases where canonical domains were not evident.

Acknowledgements

This work was partially supported by NASA (80NSSC18K1067) to AHW and MQM and NSF (1755364) to MQM. We thank Ryan Christopher Vignogna, Lin Luan, Le Li and Brian Walters for help with AlphaFold analysis.

References

1. Holzem, M., Boutros, M. & Holstein, T. W. The origin and evolution of Wnt signalling. *Nat Rev Genet* **25**, 500–512 (2024).
2. Petersen, C. P. & Reddien, P. W. Wnt signaling and the polarity of the primary body axis. *Cell* **139**, 1056–1068 (2009).
3. Wikramanayake, A. H. *et al.* An ancient role for nuclear β-catenin in the evolution of axial polarity and germ layer segregation. *Nature* **426**, 446–450 (2003).
4. Rim, E. Y., Clevers, H. & Nusse, R. The Wnt Pathway: From Signaling Mechanisms to Synthetic Modulators. *Annu Rev Biochem* **91**, 571–598 (2022).
5. Clevers, H., Loh, K. M. & Nusse, R. Stem cell signaling. An integral program for tissue renewal and regeneration: Wnt signaling and stem cell control. *Science* **346**, 1248012 (2014).
6. Richards, G. S. & Degnan, B. M. The dawn of developmental signaling in the metazoa. *Cold Spring Harb Symp Quant Biol* **74**, 81–90 (2009).
7. Babonis, L. S. & Martindale, M. Q. Phylogenetic evidence for the modular evolution of metazoan signalling pathways. *Philosophical Transactions of the Royal Society B: Biological Sciences* **372**, 20150477 (2017).
8. Gammons, M. & Bienz, M. Multiprotein complexes governing Wnt signal transduction. *Curr Opin Cell Biol* **51**, 42–49 (2018).
9. MacDonald, B. T., Tamai, K. & He, X. Wnt/β-Catenin Signaling: Components, Mechanisms, and Diseases. *Developmental Cell* **17**, 9–26 (2009).
10. Liu, J. *et al.* Wnt/β-catenin signalling: function, biological mechanisms, and therapeutic opportunities. *Sig Transduct Target Ther* **7**, 1–23 (2022).

11. Valenta, T., Hausmann, G. & Basler, K. The many faces and functions of β-catenin. *EMBO J* **31**, 2714–2736 (2012).

12. Schippers, K. J. & Nichols, S. A. Evidence of Signaling and Adhesion Roles for β-Catenin in the Sponge Ephydatia muelleri. *Molecular Biology and Evolution* **35**, 1407–1421 (2018).

13. Lee, P. N., Kumburegama, S., Marlow, H. Q., Martindale, M. Q. & Wikramanayake, A. H. Asymmetric developmental potential along the animal-vegetal axis in the anthozoan cnidarian, Nematostella vectensis, is mediated by Dishevelled. *Dev Biol* **310**, 169–186 (2007).

14. Martindale, M. Q. & Hejnol, A. A developmental perspective: changes in the position of the blastopore during bilaterian evolution. *Dev Cell* **17**, 162–174 (2009).

15. Schneider, S. Q., Finnerty, J. R. & Martindale, M. Q. Protein evolution: structure-function relationships of the oncogene beta-catenin in the evolution of multicellular animals. *J Exp Zool B Mol Dev Evol* **295**, 25–44 (2003).

16. Roberts, D. M. *et al.* Deconstructing the β-catenin destruction complex: mechanistic roles for the tumor suppressor APC in regulating Wnt signaling. *Mol Biol Cell* **22**, 1845–1863 (2011).

17. Stamos, J. L. & Weis, W. I. The β-catenin destruction complex. *Cold Spring Harb Perspect Biol* **5**, a007898 (2013).

18. van Kappel, E. C. & Maurice, M. M. Molecular regulation and pharmacological targeting of the β-catenin destruction complex. *Br J Pharmacol* **174**, 4575–4588 (2017).

19. Fagotto, F. *et al.* Domains of Axin Involved in Protein–Protein Interactions, Wnt Pathway Inhibition, and Intracellular Localization. *J Cell Biol* **145**, 741–756 (1999).

20. Kishida, S. *et al.* Axin, a Negative Regulator of the Wnt Signaling Pathway, Directly Interacts with Adenomatous Polyposis Coli and Regulates the Stabilization of β-Catenin. *Journal of Biological Chemistry* **273**, 10823–10826 (1998).

21. Ikeda, S. *et al.* Axin, a negative regulator of the Wnt signaling pathway, forms a complex with GSK-3beta and beta-catenin and promotes GSK-3beta-dependent phosphorylation of beta-catenin. *EMBO J* **17**, 1371–1384 (1998).

22. Qiu, L. *et al.* The scaffold protein AXIN1: gene ontology, signal network, and physiological function. *Cell Communication and Signaling* **22**, 77 (2024).

23. Pronobis, M. I., Rusan, N. M. & Peifer, M. A novel GSK3-regulated APC:Axin interaction regulates Wnt signaling by driving a catalytic cycle of efficient βcatenin destruction. *eLife* https://elifesciences.org/articles/08022 (2015) doi:10.7554/eLife.08022.

24. Ranes, M., Zaleska, M., Sakalas, S., Knight, R. & Guettler, S. Reconstitution of the destruction complex defines roles of AXIN polymers and APC in β-catenin capture, phosphorylation, and ubiquitylation. *Mol Cell* **81**, 3246-3261.e11 (2021).

25. Xing, Y., Clements, W. K., Kimelman, D. & Xu, W. Crystal structure of a β-catenin/Axin complex suggests a mechanism for the β-catenin destruction complex. *Genes Dev.* **17**, 2753–2764 (2003).

26. Liu, C. *et al.* Control of beta-catenin phosphorylation/degradation by a dual-kinase mechanism. *Cell* **108**, 837–847 (2002).

27. Kimelman, D. & Xu, W. beta-catenin destruction complex: insights and questions from a structural perspective. *Oncogene* **25**, 7482–7491 (2006).

28. Richter, D. J., Fozouni, P., Eisen, M. B. & King, N. Gene family innovation, conservation and loss on the animal stem lineage. *eLife* **7**, e34226 (2018).

29. Kumburegama, S., Wijesena, N., Xu, R. & Wikramanayake, A. H. Strabismus-mediated primary archenteron invagination is uncoupled from Wnt/β-catenin-dependent endoderm cell fate specification in Nematostella vectensis (Anthozoa, Cnidaria): Implications for the evolution of gastrulation. *EvoDevo* **2**, 2 (2011).

30. Kraus, Y., Aman, A., Technau, U. & Genikhovich, G. Pre-bilaterian origin of the blastoporal axial organizer. *Nat Commun* **7**, 11694 (2016).

31. Lee, P. N., Pang, K., Matus, D. Q. & Martindale, M. Q. A WNT of things to come: evolution of Wnt signaling and polarity in cnidarians. *Semin Cell Dev Biol* **17**, 157–167 (2006).

32. Houliston, E., Momose, T. & Manuel, M. Clytia hemisphaerica: a jellyfish cousin joins the laboratory. *Trends Genet* **26**, 159–167 (2010).

33. Layden, M. J., Rentzsch, F. & Röttinger, E. The rise of the starlet sea anemone Nematostella vectensis as a model system to investigate development and regeneration. *Wiley Interdiscip Rev Dev Biol* **5**, 408–428 (2016).

34. Adamska, M. *et al.* Structure and expression of conserved Wnt pathway components in the demosponge Amphimedon queenslandica. *Evol Dev* **12**, 494–518 (2010).

35. Abbott, J. & Näthke, I. S. The adenomatous polyposis coli protein 30 years on. *Semin Cell Dev Biol* **150–151**, 28–34 (2023).

36. Jumper, J. *et al.* Highly accurate protein structure prediction with AlphaFold. *Nature* **596**, 583–589 (2021).

37. Abramson, J. *et al.* Accurate structure prediction of biomolecular interactions with AlphaFold 3. *Nature* **630**, 493–500 (2024).

38. Bryant, P., Pozzati, G. & Elofsson, A. Improved prediction of protein-protein interactions using AlphaFold2. *Nat Commun* **13**, 1265 (2022).

39. Röttinger, E., Dahlin, P. & Martindale, M. Q. A Framework for the Establishment of a Cnidarian Gene Regulatory Network for "Endomesoderm" Specification: The Inputs of ß-Catenin/TCF Signaling. *PLOS Genetics* **8**, e1003164 (2012).

40. Lebedeva, T. *et al.* Cnidarian-bilaterian comparison reveals the ancestral regulatory logic of the β-catenin dependent axial patterning. *Nat Commun* **12**, 4032 (2021).

41. Wijesena, N., Sun, H., Kumburegama, S. & Wikramanayake, A. H. Distinct Frizzled receptors independently mediate endomesoderm specification and primary archenteron invagination during gastrulation in *Nematostella*. *Developmental Biology* **481**, 215–225 (2022).

42. Servetnick, M. D. *et al.* Cas9-mediated excision of Nematostella brachyury disrupts endoderm development, pharynx formation and oral-aboral patterning. *Development* **144**, 2951–2960 (2017).

43. Sun, H., Peng, C. J., Wang, L., Feng, H. & Wikramanayake, A. H. An early global role for Axin is required for correct patterning of the anterior-posterior axis in the sea urchin embryo. *Development* **148**, dev191197 (2021).

44. Wikramanayake, A. H., Huang, L. & Klein, W. H. β-Catenin is essential for patterning the maternally specified animal-vegetal axis in the sea urchin embryo. *Proceedings of the National Academy of Sciences* **95**, 9343–9348 (1998).

45. Logan, C. Y., Miller, J. R., Ferkowicz, M. J. & McClay, D. R. Nuclear β-catenin is required to specify vegetal cell fates in the sea urchin embryo. *Development* **126**, 345–357 (1999).

46. Hedgepeth, C. M., Deardorff, M. A., Rankin, K. & Klein, P. S. Regulation of glycogen synthase kinase 3beta and downstream Wnt signaling by axin. *Mol Cell Biol* **19**, 7147–7157 (1999).

47. Kremer, S. A., Erdeniz, N., Peterson-Nedry, W., Swanson, E. A. & Wehrli, M. In vivo analysis in Drosophila reveals differential requirements of contact residues in Axin for interactions with GSK3beta or beta-catenin. *Dev Biol* **337**, 110–123 (2010).

48. Chou, H.-Y. *et al.* GSKIP Is Homologous to the Axin GSK3β Interaction Domain and Functions as a Negative Regulator of GSK3β. *Biochemistry* **45**, 11379–11389 (2006).

49. Dajani, R. *et al.* Structural basis for recruitment of glycogen synthase kinase 3β to the axin–APC scaffold complex. *EMBO J* **22**, 494–501 (2003).

50. Peterson-Nedry, W. *et al.* Unexpectedly robust assembly of the Axin destruction complex regulates Wnt/Wg signaling in Drosophila as revealed by analysis in vivo. *Dev Biol* **320**, 226–241 (2008).

51. Pronobis, M. I., Deuitch, N., Posham, V., Mimori-Kiyosue, Y. & Peifer, M. Reconstituting regulation of the canonical Wnt pathway by engineering a minimal β-catenin destruction machine. *Mol Biol Cell* **28**, 41–53 (2017).

52. Ha, N.-C., Tonozuka, T., Stamos, J. L., Choi, H.-J. & Weis, W. I. Mechanism of phosphorylation-dependent binding of APC to beta-catenin and its role in beta-catenin degradation. *Mol Cell* **15**, 511–521 (2004).

53. Villalobos, V. *et al.* Dual-Color Click Beetle Luciferase Heteroprotein Fragment Complementation Assays. *Chem Biol* **17**, 1018–1029 (2010).

54. Dunn, C. W. *et al.* Broad phylogenomic sampling improves resolution of the animal tree of life. *Nature* **452**, 745–749 (2008).

55. Schultz, D. T. *et al.* Ancient gene linkages support ctenophores as sister to other animals. *Nature* **618**, 110–117 (2023).

56. Yang, J. *et al.* Adenomatous polyposis coli (APC) differentially regulates beta-catenin phosphorylation and ubiquitination in colon cancer cells. *J Biol Chem* **281**, 17751–17757 (2006).

57. Polakis, P. Mutations in the APC gene and their implications for protein structure and function. *Current Opinion in Genetics & Development* **5**, 66–71 (1995).

58. Soyer, O. S. & Bonhoeffer, S. Evolution of complexity in signaling pathways. *Proceedings of the National Academy of Sciences* **103**, 16337–16342 (2006).

59. Bince, J. M. & Wikramanayake, A. H. Functional analysis of Wnt signaling in the early sea urchin embryo using mRNA microinjection. *Methods Mol Biol* **469**, 213–222 (2008).

60. Salinas-Saavedra, M., Rock, A. Q. & Martindale, M. Q. Germ layer-specific regulation of cell polarity and adhesion gives insight into the evolution of mesoderm. *Elife* **7**, e36740 (2018).

Figures

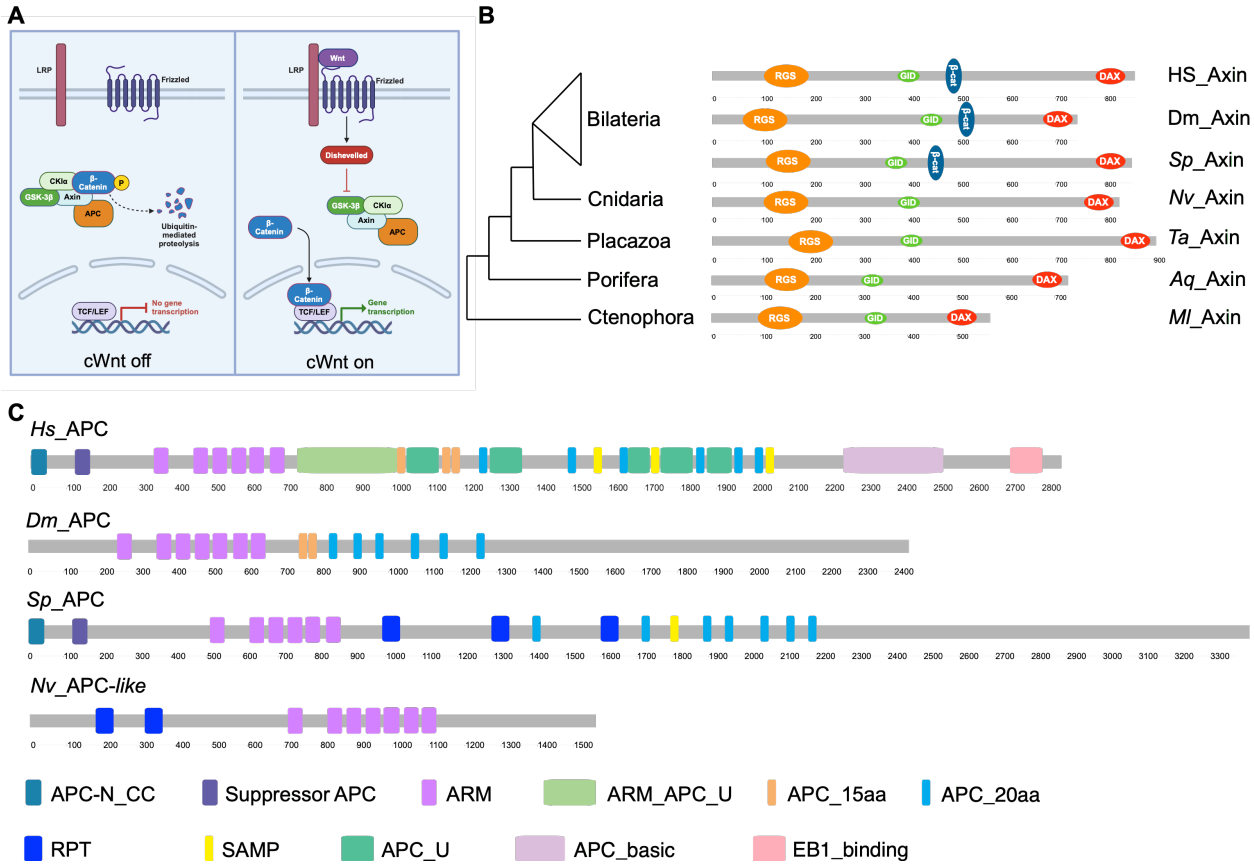

Figure 1- The Wnt/ β-catenin (cWnt) pathway and a phylogenetic overview of the evolution of protein-protein interaction domains in the scaffolding proteins Axin and APC. (A) Simplified representation of the cWnt pathway in its "off "and "on" states, showing the activity of the destruction complex scaffolded by the Axin and APC proteins. (B) A simplified phylogenetic tree showing the evolutionary relationship between Bilateria and non-Bilateria taxa comparing the main protein binding domains of Axin in bilaterians and non-bilaterians. (C) Schematic diagram of APC protein domain structures in bilaterians and non-bilaterian. *Hs*, *Homo sapiens*; *Dm*, *Drosophila melanogaster*; *Sp*, *Strongylocentrotus purpuratus*; *Nv*, *Nematostella vectensis*; *Ta*, *Trichoplax adhaerens*; *Aq*, *Amphimedon queenslandica*; *Ml*, *Mnemiopsis leidyi*. The numbers under the protein structures indicate the amino acid position. The color codes for the domains are indicated within or below the protein structures.

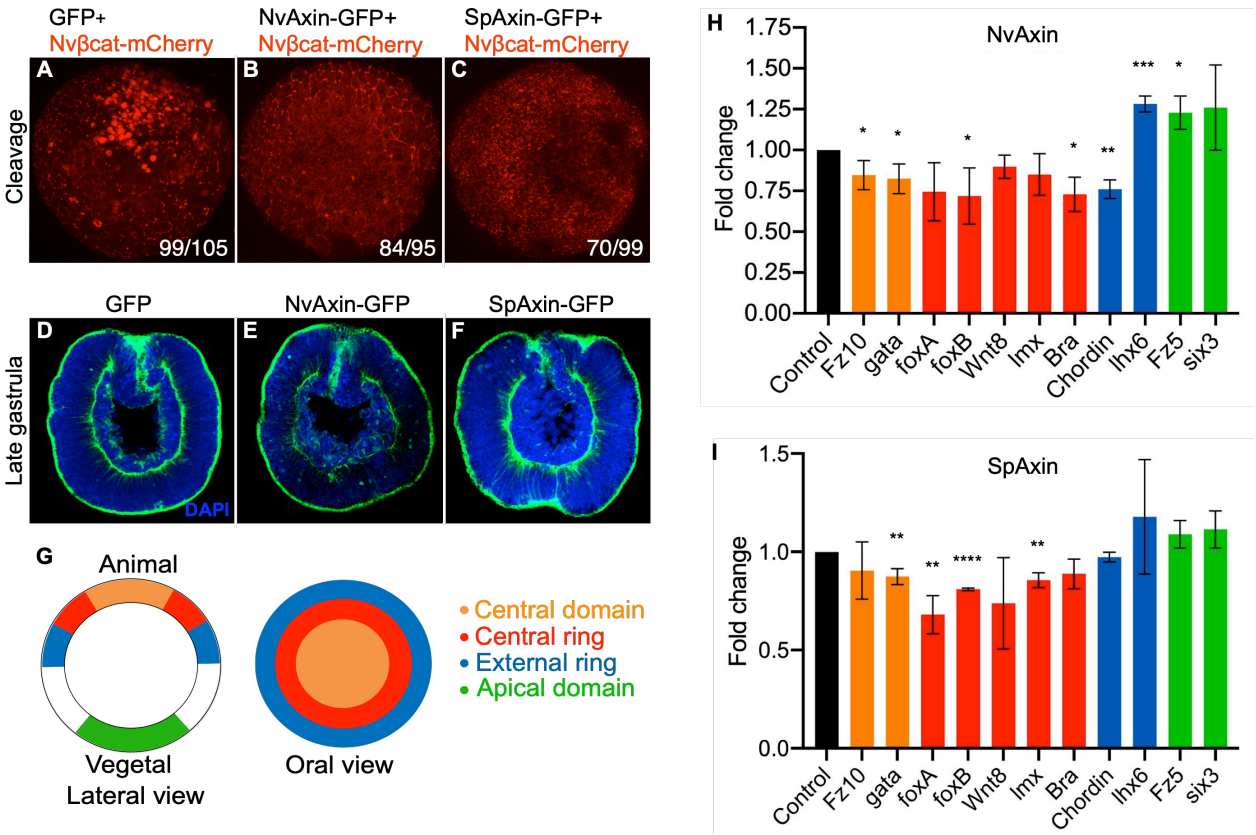

Figure 2- Overexpression of NvAxin in *Nematostella* embryos disrupts Wnt/β-catenin signaling. In the control, co-overexpression of GFP and Nvβ-catenin-mCherry showed that β-catenin-mCherry was enriched in the nuclei at one side of the embryo (A). However, co-overexpression of NvAxin-GFP (B) or SpAxin-GFP (C) with Nvβ-catenin-mCherry eliminated the nuclearization of β-catenin-mCherry. (D-F) Compared to GFP overexpressing control embryos which had a well-formed endodermal layer (D), NvAxin-GFP overexpressing embryos (E) and sea urchin Axin overexpressing embryos (SpAxin-GFP) (F) initiated primary invagination but failed to maintain a normal archenteron epithelium at the late gastrula stage. Green: phalloidin; Blue: DAPI. (G) Gene syn-expression domains as defined in Röttinger et al. (2012). Figure on the left shows a lateral view, and the figure on the right shows the oral view. (H,I) qPCR analyses of NvAxin or SpAxin overexpressing embryos at 24 hpf (hours post fertilization) showed that all endomesoderm gene markers (orange, and red bars) and pharynx markers (blue bars) were downregulated, except for lhx6. The values represent the fold change relative to the GFP control (black bars). The qPCR experiments were replicated with three separate batches of embryos, with three technical replicates in each experiment. Statistical significance was determined using the Unpaired t test. ****, $p<0.0001$; ***, $p<0.001$; **, $p<0.01$; *, $p<0.05$; n=3.

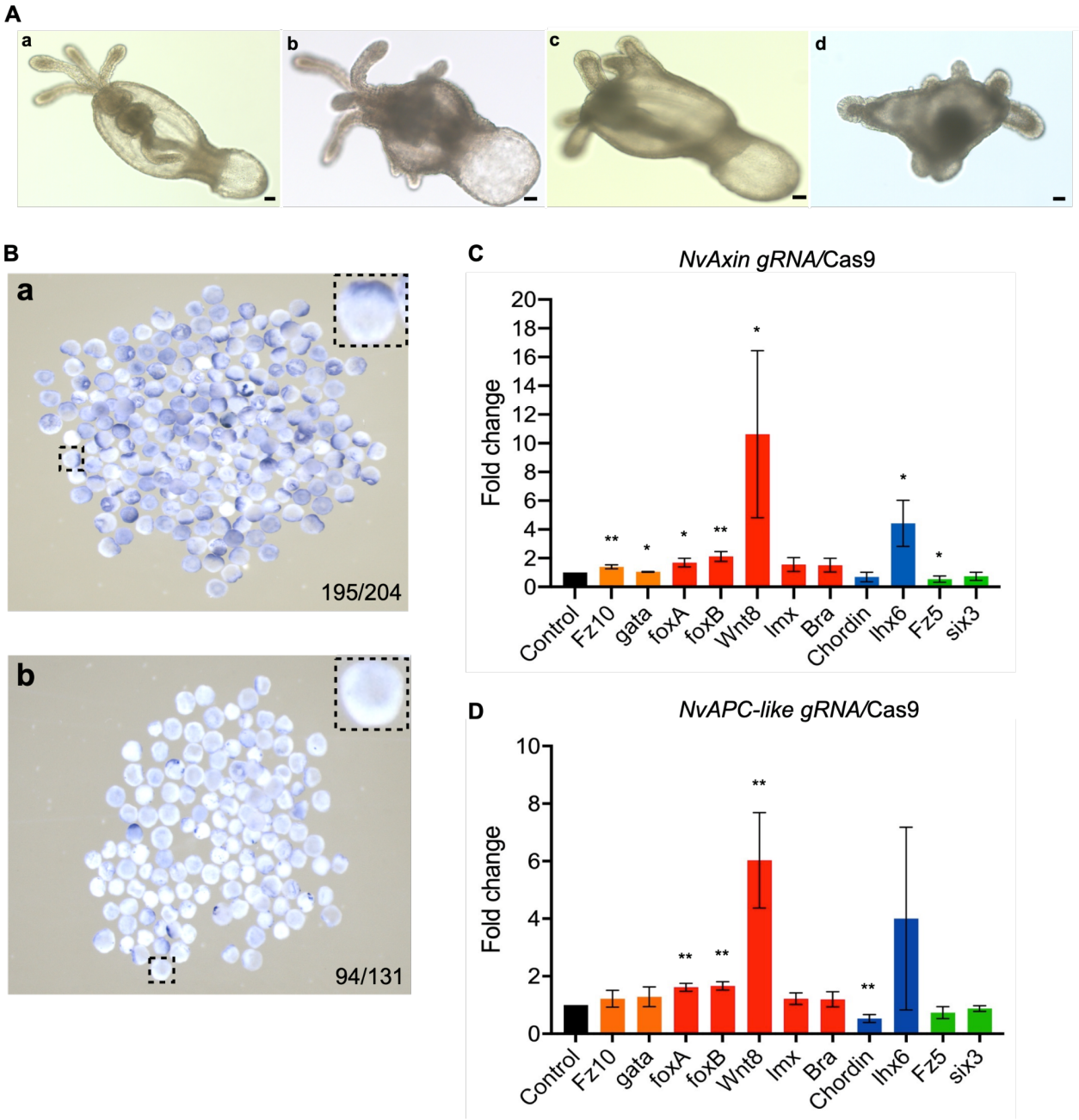

Figure 3- CRISPR/Cas9 mediated knockout of Axin and APC-like induces ectopic tentacles and upregulates endomesoderm gene expression in *Nematostella* embryos. (A) Nematostella 4-tentacle polyp, 7 days post-fertilization (7dpf) injected with Cas9 at the zygote stage (a). *NvAxin* guide RNA/Cas9 (NvAxin/gRNA) injected polyps produced ectopic tentacles (b), which is similar to *NvAPC-like* gRNA/Cas9 injected polyps (c). Co-injection of *Axin* and *APC-like* gRNA/Cas9 produced a more severe phenotype (d) than *Axin* or *APC-like* gRNA/Cas9 single injections. Scale bar = 20µm. For each injection experiment, 100-200 embryos were injected with either gRNA/Cas9 or Cas9 alone. Among these, 70-75% of the

gRNA/Cas9-injected embryos and more than 95% Cas9 only injected embryos exhibited the same morphology as shown in the representative figures. (B) While Cas9-injected embryos have normal oral pole Axin localization (a, blue staining), in situ hybridization showed that NvAxin/Cas9 injected embryos displayed reduced Axin expression (b). WMISH showed that 81.9% of the control embryos showed strong NvAxin expression at the animal pole; 13.7% showed detectable but weaker asymmetrical NvAxin expression, and 4.4% showed no detectable signal (n=204)(Fig. 2Ba). By contrast, 72.5% of NvAxin gRNA/Cas9-injected embryos showed no detectable Axin expression, 24.4% showed weak Axin expression, and only 3.1% showed a signal like that seen in the control (n=131)(Fig. 2Bb). The embryos with weak NvAxin signals may be due to incomplete excision of NvAxin or the generation of mosaic embryos where the gene was only excised in some nuclei. (C and D) qPCR shows the effects of Axin and APC-like knock-out by CRISPR/Cas9 on the expression of endomesoderm and pharynx gene markers. Fz10, gata, foxA, foxB, Wnt8, lmx, Brachyury (Bra) (orange and red bars) are endo mesodermal markers, Chordin, lhx6 (blue bars) are markers for the pharynx; Fz5 and six3 (green bars) are ectoderm gene makers. qPCR experiments were replicated with three separate batches of embryos with three technical replicates in each experiment. Graphs shown fold change in mRNA levels normalized to the Cas9 only control (black bars). Statistical significance was determined using the Unpaired t test. **, $p<0.01$; *, $p<0.05$; n=3.

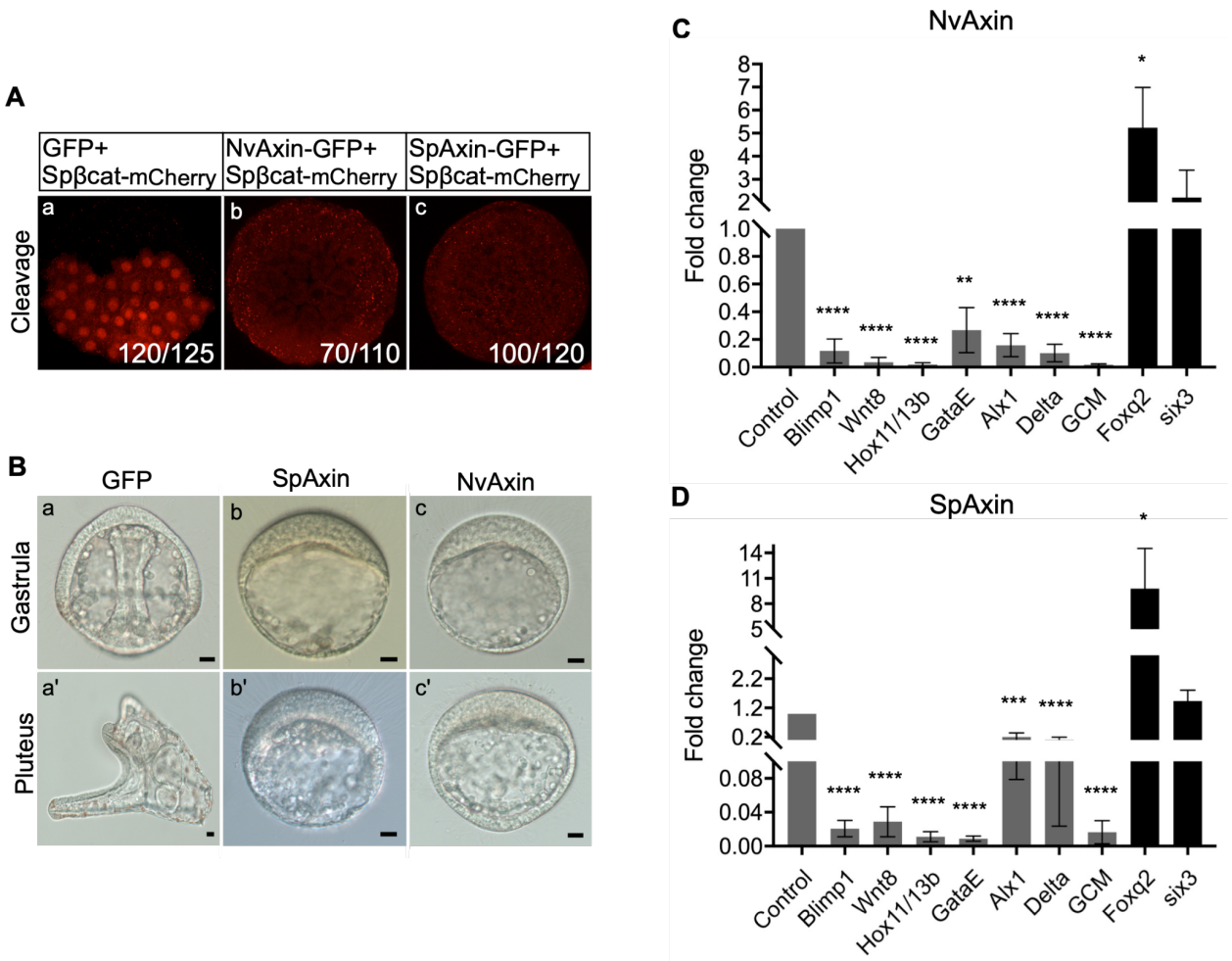

Figure 4- Overexpression of *Nematostella* Axin in sea urchin embryos blocked nuclearization of β-catenin and anteriorized embryos. (A) In the control where GFP and Spβ-catenin-mCherry were co-expressed, β-catenin was enriched in the nuclei at the vegetal pole (a). Co-overexpression of NvAxin (b) or SpAxin (c) with Spβ-catenin-mCherry downregulated the nuclearization of β-catenin. (B) Control embryos injected with GFP mRNA developed normally (a, a'), while embryos developing from SpAxin or NvAxin mRNA-injected zygotes became severely anteriorized (b, b' and c, c'). Scale bar = 10μm. (C and D) qPCR analyses showed that NvAxin or SpAxin overexpressing embryos downregulated endomesoderm genes and upregulated neuroectoderm genes. The bar graph shows the fold change of each gene between *Axin* mRNA-injected and *GFP* mRNA-injected control embryos. *Blimp1*, *Wnt8*, *Hox11/13b*, *GataE*, *Alx1*, *Delta* and *GCM* are endomesoderm gene markers; *Foxq2* and *Six3* are neuroectoderm gene markers. qPCR experiments were replicated with three separate batches of embryos with three technical replicates in each experiment. Statistical significance was determined using the Unpaired t test. ****, $p<0.0001$; ***, $p<0.001$; **, $p<0.01$; *, $p<0.05$; n=3. For each injection experiment, 200-300 embryos were injected with each construct and more than 95% of embryos had the same morphology as shown in the representative figures.

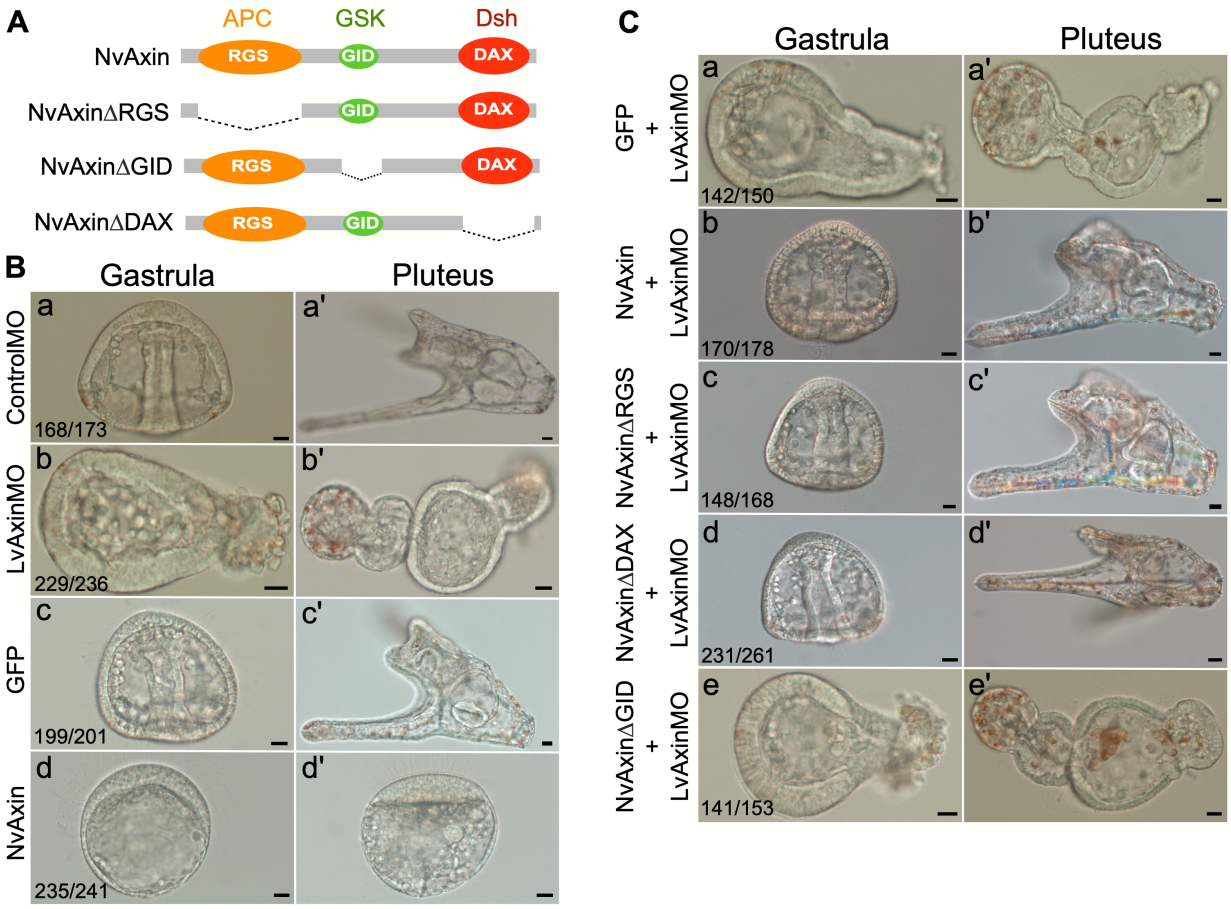

Figure 5- Sea urchin embryos posteriorized by Axin knock-down can be rescued by full-length NvAxin, NvAxinΔRGS, and NvAxinΔDAX, but not NvAxinΔGID. (A) Schematic representations of full-length Axin and domain-deletion constructs. (B) Gastrula and pluteus larva developing from Control MO, LvAxin MO, *GFP* mRNA or *NvAxin* mRNA injected zygotes from the sea urchin *Lytechinus variegatus* (a-d'). Control MO-injected embryos develop normally (a,a'), while LvAxin MO-injected embryos become posteriorized (b, b'). *GFP* mRNA-injected zygotes produce normal embryos (c, c'), while *NvAxin* mRNA-injected zygotes develop into anteriorized embryos (d, d'). (C) The posteriorized phenotype induced in LvAxin MO-injected zygote is not rescued by control *GFP* mRNA co-injection (a, a') but is rescued by the expression of NvAxin (b, b'), NvAxinΔRGS (c, c'), and NvAxinΔDAX (d, d'). Injection of *NvAxinΔGID* mRNA fails to rescue the posteriorization induced by Axin knockdown (e,e'). Scale bar = 10 µm. The numbers in the panels indicate the number of embryos examined and the number that showed the phenotype.

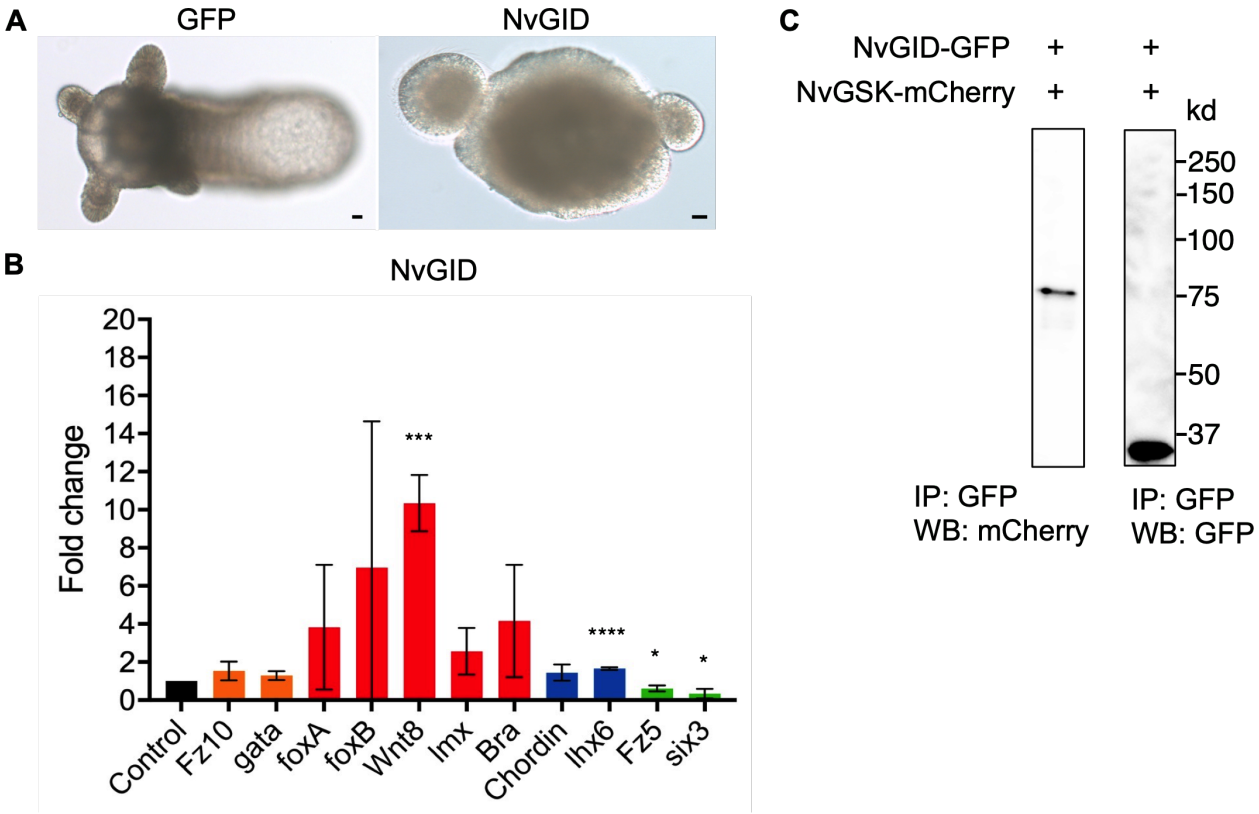

Figure 6- Overexpression of the NvAxin GID domain upregulated endomesodermal and pharyngeal gene expression in *Nematostella* embryos. (A) Comparison of animals developing from *Nematostella* zygotes injected with *GFP* mRNA (control) or *NvAxin-GID (NvGID)* mRNA at 7 days post fertilization (7dpf). At 7dpf control animals were at the polyp stage while *NvGID* RNA-injected embryos developed abnormally. Scale bar =10 µm. (B) qPCR analyses of NvGID overexpressing embryos at 24 hpf (hours post fertilization) showed that all endomesoderm gene markers (orange, red and blue bars) were upregulated. Some genes were unregulated at modest levels while others showed significant increases. The two apical domain genes were significantly downregulated. The qPCR experiments were replicated with three separate batches of embryos, with three technical replicates in each experiment. Graphs shown fold change in mRNA levels normalized to the GFP control (black bars). Statistical significance was determined using the Unpaired t test. ****, $p<0.0001$; ***, $p<0.001$; *, $p<0.05$; n=3. (C) Western blot analysis of anti-GFP antibody-mediated immunoprecipitation of *in vitro* synthesized NvGID-GFP and NvGSK-3β-mCherry fused proteins.

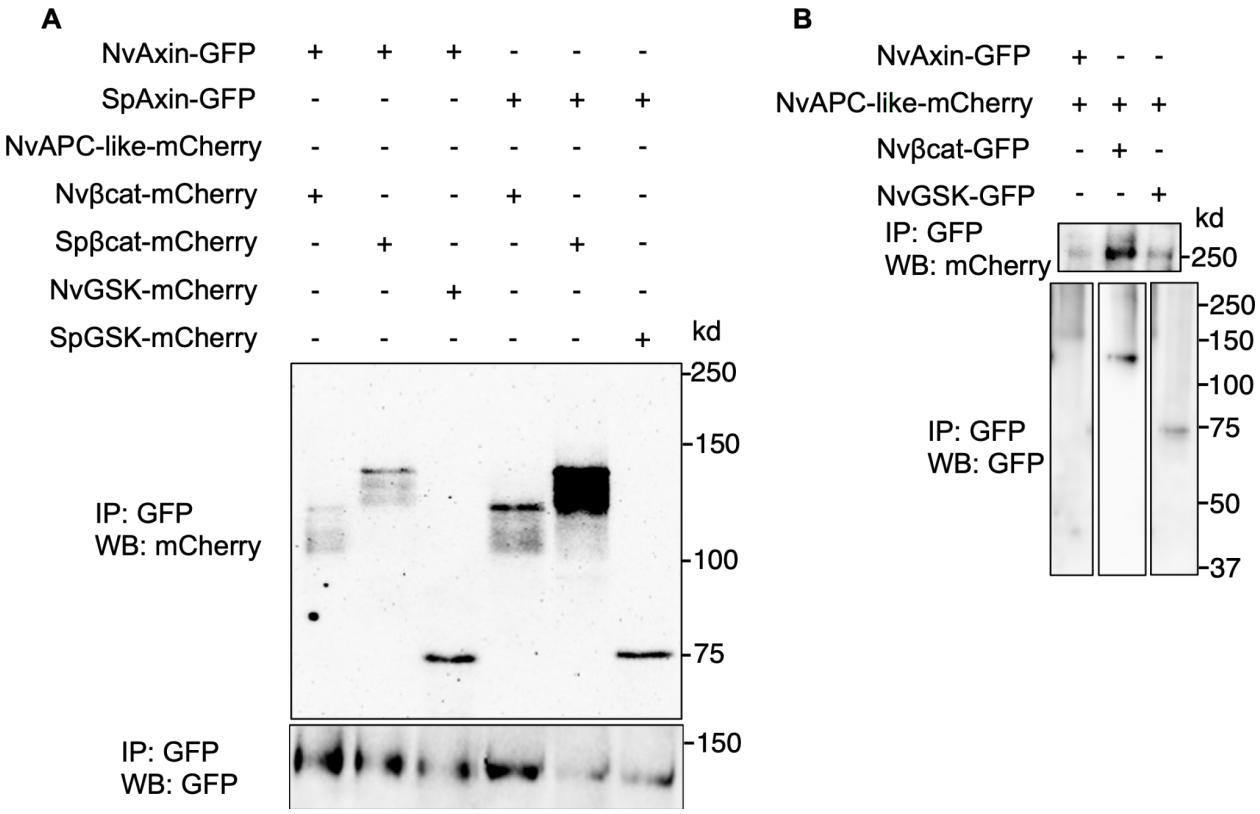

Figure 7- *In vitro* analysis of protein-protein interactions between Nvβ-catenin and components of the β-catenin destruction complex.
(A) *In vitro*-synthesized GFP- or mCherry-fused proteins were tested for potential interactions by mixing a GFP-fused partner with a mCherry-fused partner and performing immunoprecipitation (IP) with an anti-GFP antibody. The labels at the top of the panel show the interacting proteins in each experiment. The top part of the Western blot analysis shows the protein-protein interactions between protein pairs. The bottom part of the figure shows the GFP-tagged proteins. Sea urchin (*Strongylocentrotus purpuratus*) β-catenin (Spβ-catenin) shows a strong interaction with sea urchin Axin (SpAxin) (Lane 5), while Nvβ-catenin shows a consistent but considerably weaker interaction with NvAxin (Lane 1). NvAxin also shows a relatively weaker interaction with Spβ-catenin (compare lanes 2 and 5). Unexpectedly, SpAxin shows a weaker interaction with Nvβ-catenin than with SpAxin (compare lane 4 and lane 5). Sp and Nv Axin bind the SpGSK-3β and NvGSK-3β respectively (lanes 3 and 6). (B) NvAPC-like and Nvβ-catenin interact strongly in vitro (lane 2) while NvAPC-like shows weaker but consistent interactions with NvAxin and NvGSK-3β (lanes 1 and 3).

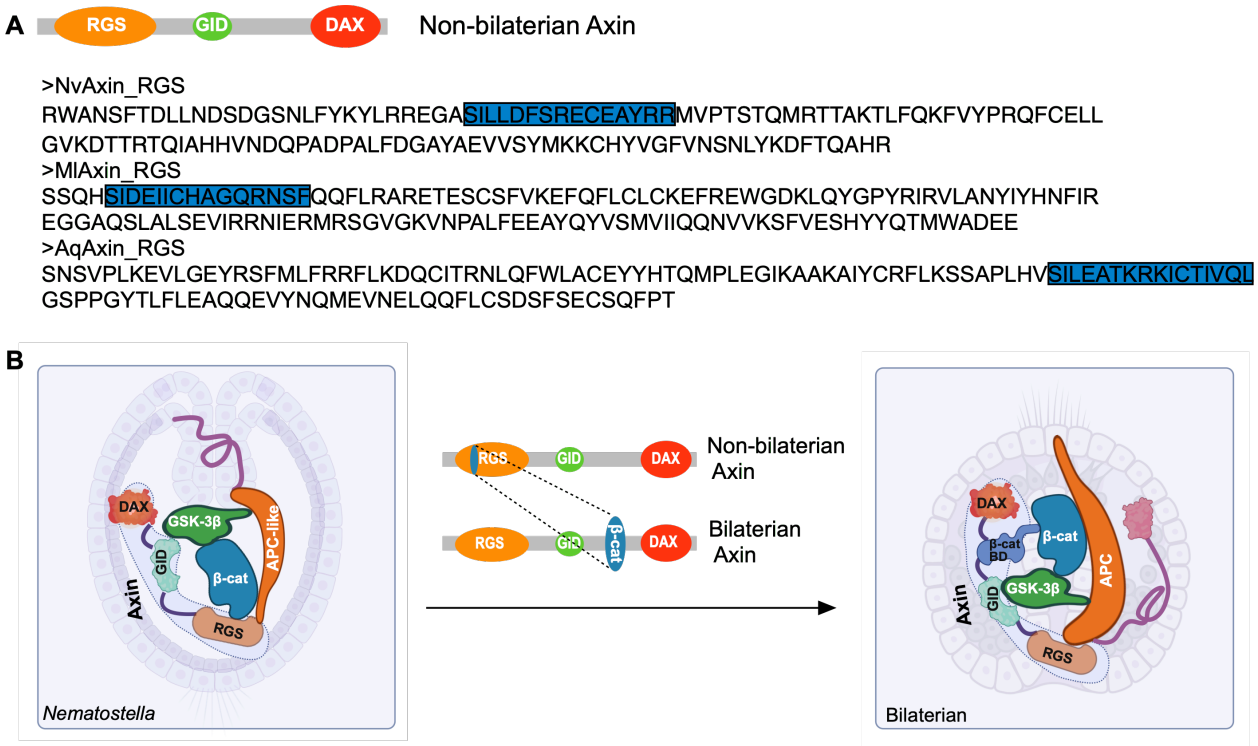

Figure 8- A hypothetical model for the evolution of the β-catenin destruction complex in bilaterians. (A) Bioinformatic predictions indicate that an amino acid sequence similar to the bilaterian β-catenin-binding motif is embedded in the RGS domain of non-bilaterian Axin. The domain structure is shown at the top and sequences of the Axin RGS domains are displayed below. The predicted β-catenin-binding region in each sequence is highlighted in blue. (B) Comparative models of the β-catenin destruction complex in cnidarians (inferred from work in *Nematostella*)and bilaterians. In *Nematostella*, β-catenin binds to an APC-like protein, while GSK-3β binds to Axin, forming a functional destruction complex. *In vitro* protein-protein interaction experiments and bioinformatic predictions suggest a low-affinity interaction between *Nematostella* β-catenin and a putative β-catenin-binding motif within the RGS domain of NvAxin. In bilaterians, β-catenin binds to both Axin, via a β-catenin-binding domain, and interacts with APC in the destruction complex. Interaction with both Axin and APC are required for regulating β-catenin phosphorylation and degradation. Models were created using BioRender.

Supplementary Table 1. The primary protein interaction domains on Axin proteins from bilaterian and non-bilaterian taxa. In bilaterians (black), Axin proteins contain APC- (RGS), GSK-3β- (GID), β-catenin- (β-cat), and Disheveled- (DAX) binding domains. In non-bilaterians (red), the conserved β-catenin binding domain between the GID and DAX domains is absent.

Species Name & Accession # / Axin Domains	RGS	GID	β-cat	DAX
Strongylocentrotus purpuratus (XP_003729076)	✓	✓	✓	✓
Saccoglossus kowalevskii (NP_001158475)	✓	✓	✓	✓
Platynereis dumerilii (ANS60441)	✓	✓	✓	✓
Crassostrea gigas (EKC24785.1)	✓	×	✓	✓
Branchiostoma floridae (XP_035695674)	✓	✓	✓	✓
Homo sapiens (NP_003493)	✓	✓	✓	✓
Mus musculus (AAC53285)	✓	✓	✓	✓
Xenopus laevis (NP_001081874)	✓	✓	✓	✓
Danio rerio (BAA92439)	✓	✓	✓	✓
Hofstenia miamia (KJ658749.1)	×	✓	✓	✓
Tribolium castaneum (NP_001280495)	✓	×	✓	✓
Drosophila melanogaster (NP_733336)	✓	✓	✓	✓
Apis mellifera (XP_006564444)	✓	✓	✓	✓
Nematostella vectensis (XP_048576223)	✓	✓	×	✓
Mnemiopsis leidyi (ML04208a)	✓	✓	×	✓
Amphimedon queenslandica (NP_001266244)	✓	✓	×	✓
Trichoplax adhaerens (XP_002109778)	✓	✓	×	✓

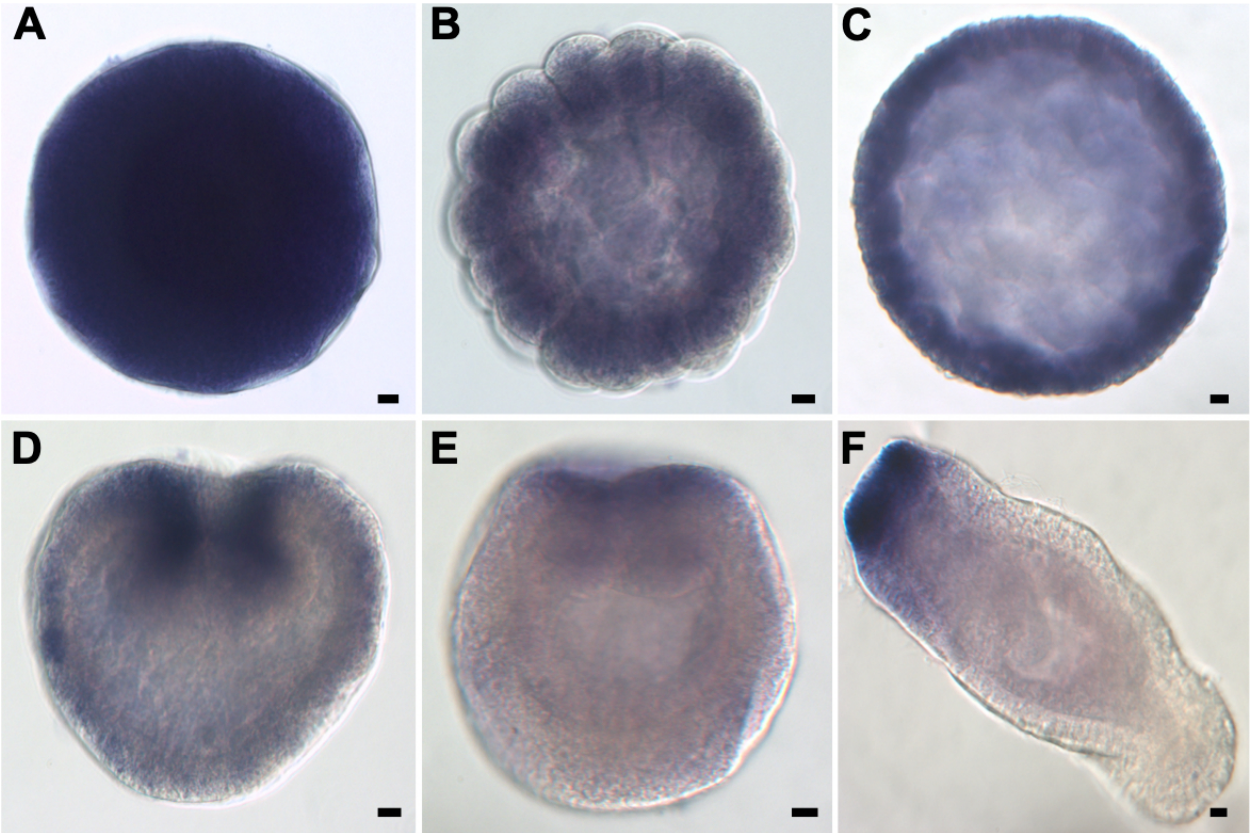

Supplementary Figure 1- Whole mount RNA in situ hybridization shows the expression of *Axin* in *Nematostella* eggs and embryos. Axin is ubiquitously expressed in the egg, and during cleavage and blastula stages (A-C), however Axin is asymmetrically expressed at the animal pole at early and late gastrula stage (D, E) and the oral side at planula stage (F). Scale bar = 10 µm.

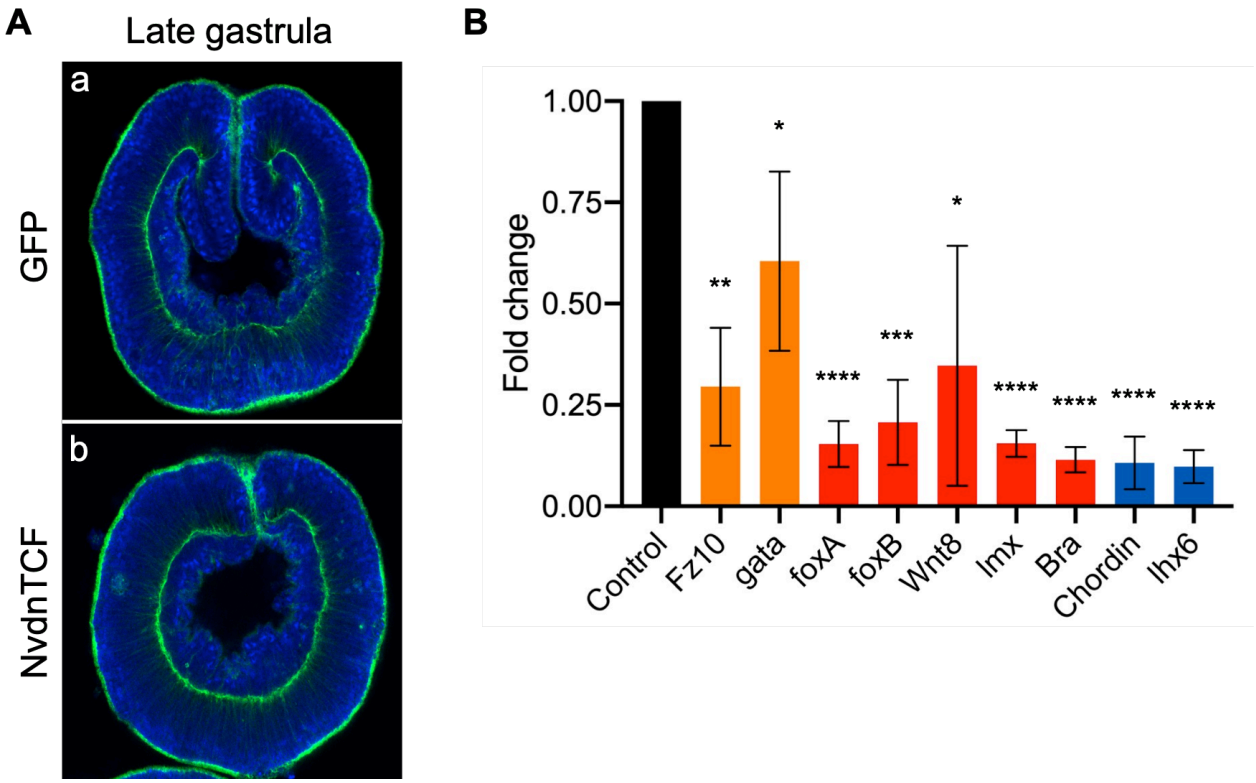

Supplementary Figure 2-The effect of NvTcf knockdown on primary invagination and endomesodermal and pharyngeal gene expression in *Nematostella* embryos. (A) Compared to GFP overexpressing control embryos (a), NvdnTCF-overexpressing embryos (b) initiated primary invagination but failed to maintain a normal archenteron epithelium at the late gastrula stage. (B) qPCR analysis of NvdnTCF-overexpressing embryos at 24 hpf (hours post fertilization) showed that all genes expressed in cells derived from animal pole blastomeres (orange, red, and blue bars) are downregulated. qPCR experiments were replicated with three separate batches of embryos with three technical replicates in each experiment. Statistical significance was determined using the Unpaired t test. ****, $p<0.0001$; ***, $p<0.001$; **, $p<0.01$; *, $p<0.05$; n=3.

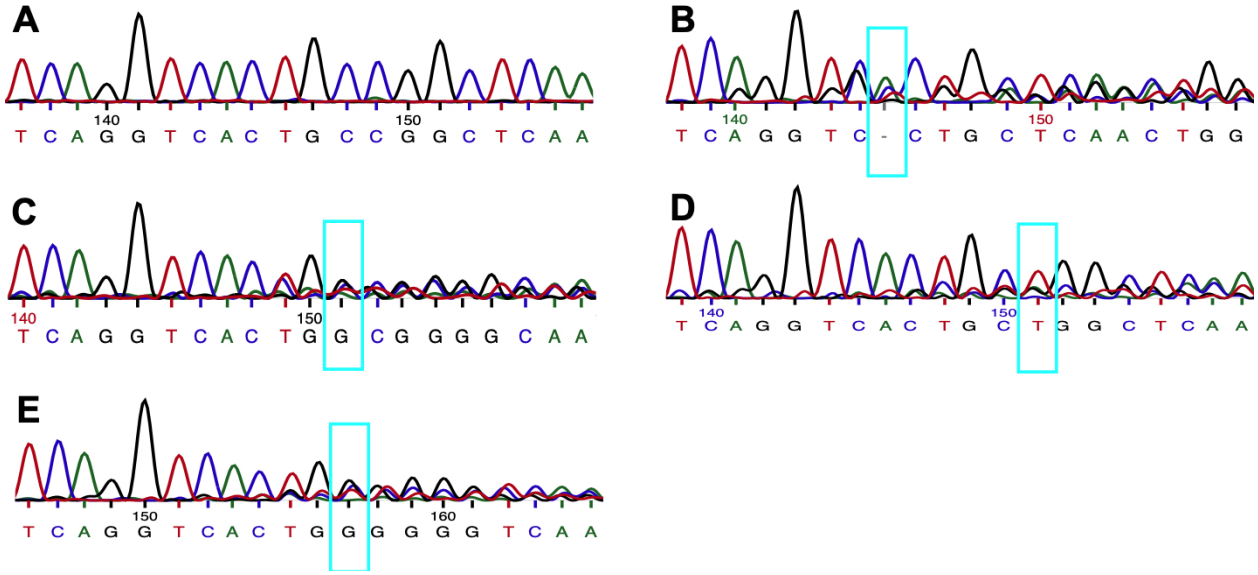

Supplementary Figure 3- Confirmation of successful CRISPR/Cas9-mediated gene editing with Sanger sequencing using a single injected embryo from each group. Compared to the Cas9 only injected embryo (A), the sequencing chromatograms showed that injection of NvAxingRNA/Cas9 induced deletions or mutations (cyan box) at the targeted region of the Axin gene (B-E).

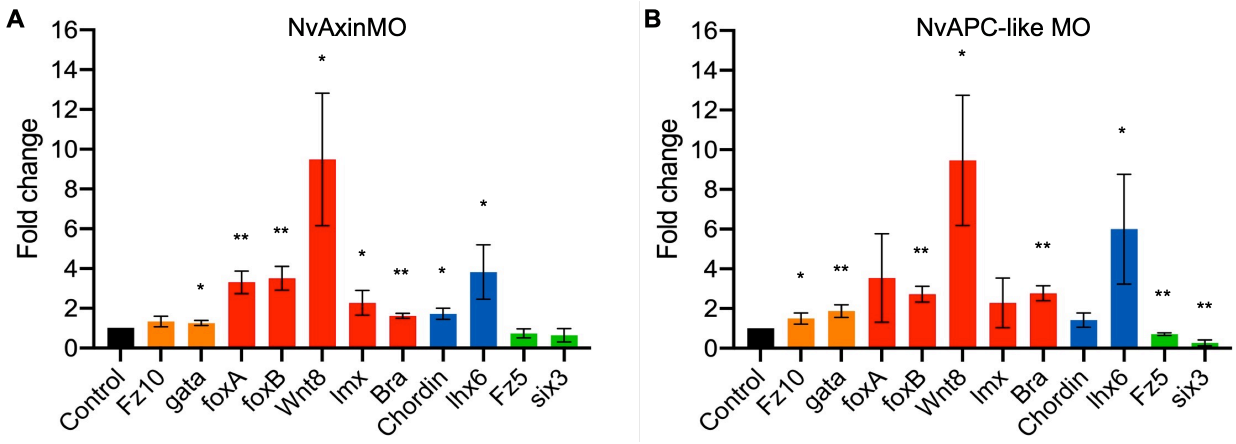

Supplementary Figure 4- Morpholino mediated knockdown of Axin or APC-like upregulates endomesoderm gene expression in *Nematostella* embryos. (A,B) Endomesoderm and pharynx gene markers were upregulated in NvAxinMO or NvAPC-like MO injected embryos compared to control MO (black bars). The qPCR experiments were replicated with three separate batches of embryos, with three technical replicates in each experiment. Statistical significance was determined using the Unpaired t test. **, $p<0.01$; *, $p<0.05$; $n=3$.

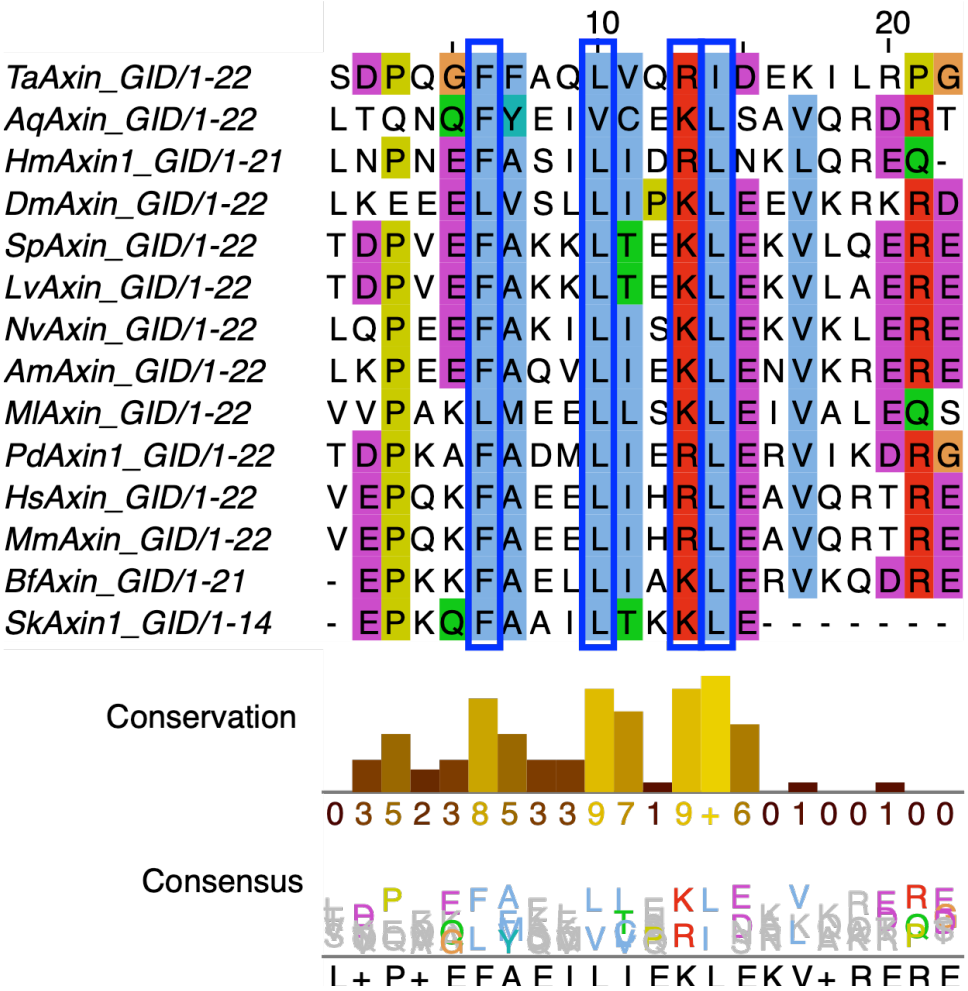

Supplementary Figure 5- The protein sequence alignment of Axin GID domains in various metazoan taxa. The top panel shows the alignments of amino acids sequence using Clustal Omega and Jalview. Conserved amino acids are highlighted in different colors, while gaps are represented in white. The bottom panel is the analysis of conservation and consensus. Ta, *Trichoplax adhaerens*; Aq, *Amphimedon queenslandica*; Hm, *Hofstenia miamia*; Dm, *Drosophila melanogaster*; Sp, *Strongylocentrotus purpuratus*; Lv, *Lytechinus variegatus*; Nv, *Nematostella vectensis*; Am, *Apis mellifera*; Ml, *Mnemiopsis leidyi*; Pd, *Platynereis dumerilii*; Hs, *Homo sapiens*; Mm, *Mus musculus*; Bf, *Branchiostoma floridae*; Sk, *Saccoglossus kowalevskii*. Blue boxes highlight the critical residues for the interactions between Axin and GSK-3β.

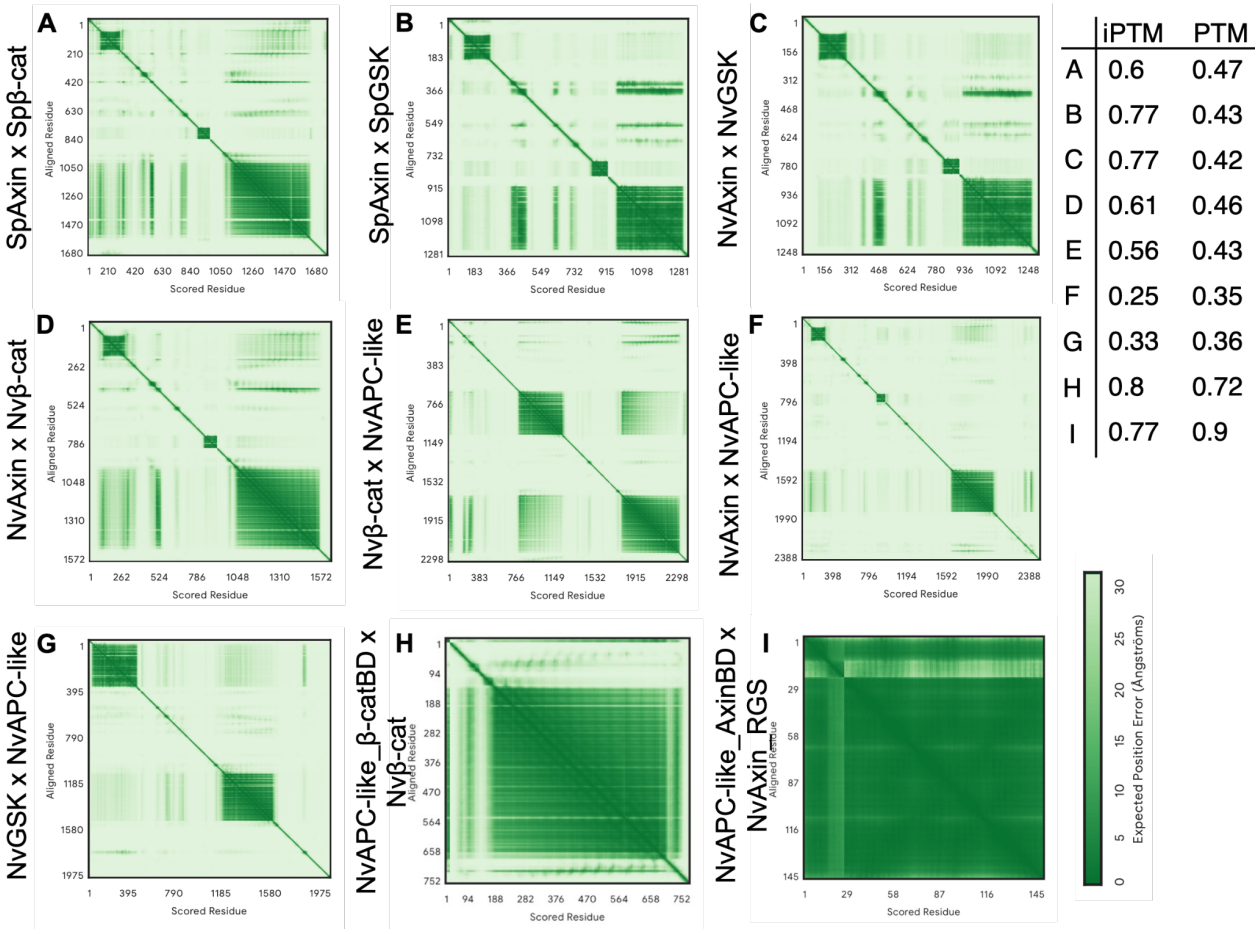

	iPTM	PTM
A	0.6	0.47
B	0.77	0.43
C	0.77	0.42
D	0.61	0.46
E	0.56	0.43
F	0.25	0.35
G	0.33	0.36
H	0.8	0.72
I	0.77	0.9

Supplementary Figure 6- AlphaFold-based predictions of protein-protein interactions between Nvβ-catenin/Spβ-catenin and components of the β-catenin destruction complex. The expected aligned error (PAE) plots for models of interactions between (A) SpAxin and Spβ-catenin (Spβ-cat), (B) SpAxin and SpGSK, (C) NvAxin and NvGSK-3β, (D) NvAxin and Nvβ-cat, (E) Nvβ-cat and NvAPC-like, (F) NvAxin and NvAPC-like, (G) NvGSK-3β and NvAPC-like, (H) NvAPC-like_β-catBD and Nvβ-cat, (I) NvAPC-like Axin binding domain (NvAPC-like_AxinBD) and NvAxin RGS. In the PAE plots, the dark green regions indicate low position error (high confidence in the relative positioning of the interacting residues), whereas light green regions indicate higher positional error (lower confidence). The iPTM and PTM scores, which represent confidence in the predicted inter-protein and intra-protein interactions, are also provided for each model.

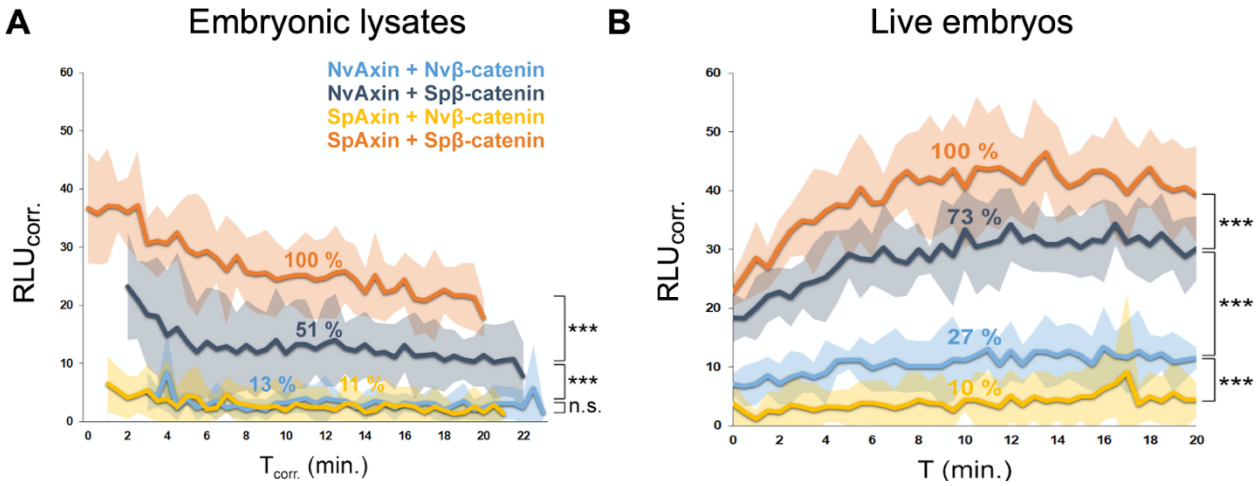

Supplementary Figure 7-The interaction of Nv- and SpAxin with Nv- or Spβ-catenin proteins in *Nematostella* embryos or embryonic lysates. Nv/SpAxin and Nv/Spβ-catenin proteins were fused to click beetle green (CBG) split luciferase fragments, and luciferase activity detected in embryo lysates (A) and live embryos(B) (n ≈ 150-300 per sample). Axin proteins were labeled C-terminally with the N-terminus of CBG (CBG-N) while β-catenin proteins were labeled N-terminally with the C-terminus of CBG (CBG-C), each connected by a flexible linker peptide. Proximity caused by protein-protein interaction results in complementation of CBG split-luc fragments into functional luciferase and hence stronger luminescence. Plots show moving averages (lines) and 95% confidence intervals (shaded areas) from three independent experiments that represent biological and technical replicates. Percentages are relative intensities compared to a combination of constructs with the strongest signal (SpAxin + Spβ-catenin) averaged across all replicates and timepoints. $RLU_{corr.}$ – intensity of luminescence in relative luciferase units normalized to the amount of expressed protein in each sample (as determined by Nanoluciferase signal). T, T_{corr} – time of measurement (corrected by the delay necessary to lyse embryos) *** $p < 0.001$, n.s. – not significant, Student's t-test.

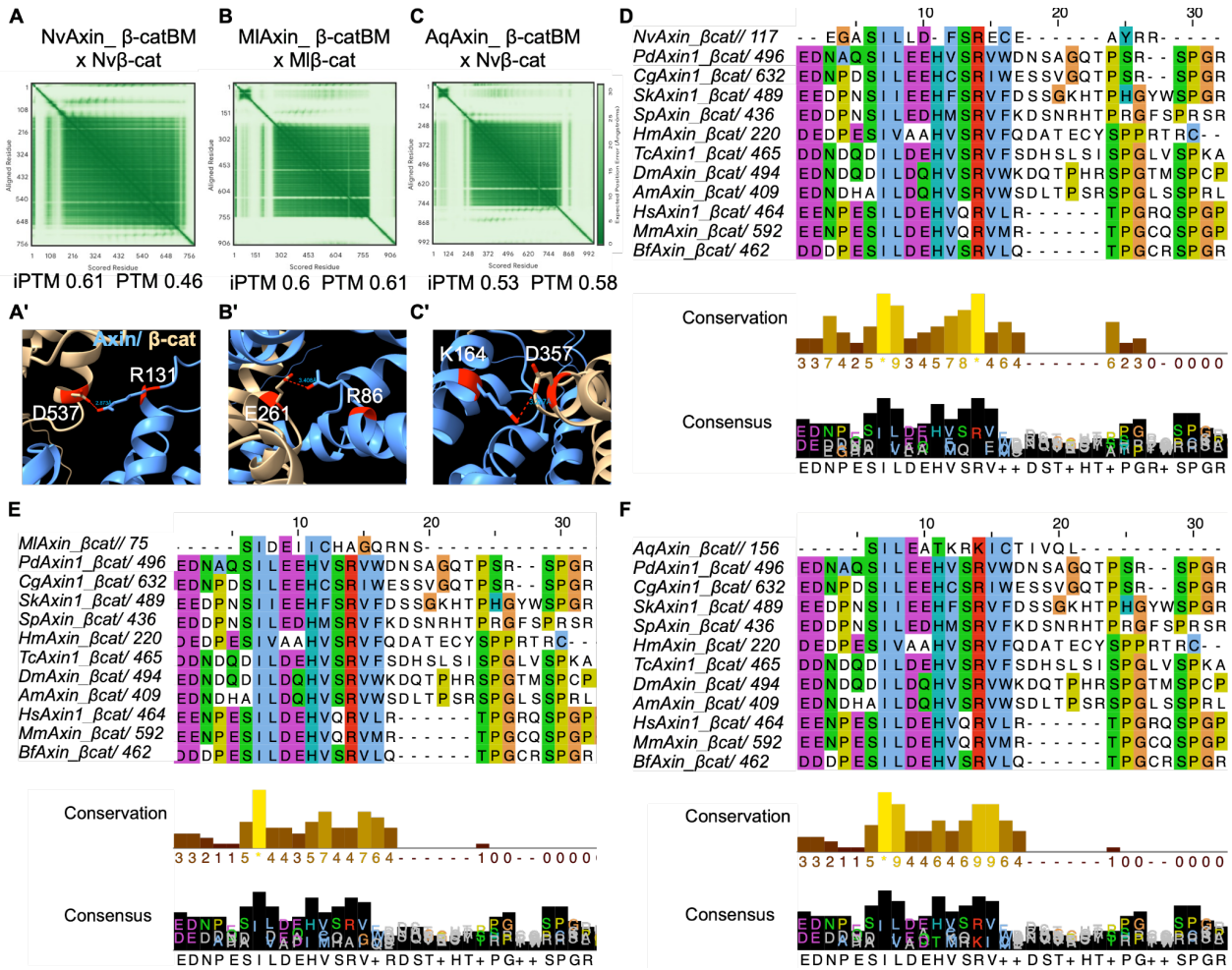

Supplementary Figure 8- Prediction of non-bilaterian Axin-β-catenin binding motif (βcatBM) using AlphaFold 3. (A-C) The Predicted Aligned Error (PAE) plots show the predicted interactions between NvAxin_βcatBM and Nvβ-catenin, MlAxin_βcatBM and Mlβ-catenin, AqAxin_βcatBM and Aqβ-catenin. In the PAE plot, dark green regions indicate low positional error (high confidence in the relative positioning of the interacting residues), while light green regions indicate higher positional error (lower confidence). The iPTM and PTM scores, which represent confidence in the predicted inter-protein and intra-protein interactions, are also provided for each model. (A'-C') Zoomed-in 3D structures of the predicted interactions between the putative *Nematostella*, *A. queenslandica*, and *M. leidyi* Axin β-catenin-binding domains and β-catenin from each species as modeled using AlphaFold. (D-F) Protein sequence alignments of various bilaterian Axin-βcatBM domains with the predicted NvAxin-βcat, MlAxin-βcat, and AqAxin-βcat motifs, respectively. Each residue in the alignment is color-coded, while gaps are shown in white. Conservation and consensus analysis are presented at the bottom of the sequence alignment. Sequence alignments were performed using Clustal Omega and Jalview . Nv, *Nematostella vectensis*; Ml, *Mnemiopsis leidyi*; Aq, *Amphimedon queenslandica*; Pd, *Platynereis dumerilii*; Cg, *Crassostrea gigas*; Sk, *Saccoglossus kowalevskii*; Sp, *Strongylocentrotus purpuratus*; Hm, *Hofstenia miamia*; Tc, *Tribolium castaneum*; Dm, *Drosophila*

melanogaster; Am, *Apis mellifera*; Hs, *Homo sapiens*; Mm, *Mus musculus*; Bf, *Branchiostoma floridae*.